Advanced Astroparticle Physics. Acceleration and Propagation of High-Energy Particles in the Universe

Version 1.1

Rafael Alves Batista
Sorbonne Université
Institut d'Astrophysique de Paris (IAP)
Lab. Physique Nucléaire et Hautes Énergies (LPNHE)
rafael.alves_batista@iap.fr

March 4, 2025

Contents

Production of high-energy particles

High-energy cosmic particles seem to be ubiquitous in the universe, spanning a wide range of energies and sources. An obvious way to produce them is to consider a Maxwellian distribution of velocities, i.e., a Maxwell-Boltzmann distribution, given by

$$f(\vec{v})\,\mathrm{d}\vec{v} = \left(\frac{m}{2\pi k_{\mathrm{B}}T}\right)^{\frac{3}{2}} \exp\left(-\frac{m|\vec{v}|^2}{2k_{\mathrm{B}}T}\right)\mathrm{d}\vec{v}\,, \tag{1.1}$$

where T the characteristic temperature of the gas of particles of mass m, and k_{B} is the Boltzmann constant. Here $f(\vec{v})$ is the probability of finding a particle with velocity between $\vec{v}$ and $\vec{v} + \mathrm{d}^3\vec{v}$.

One could think that eq. 1.1 extends to "arbitrarily high velocities", despite the exponential suppression for high speeds. However, this distribution is only valid for non-relativistic particles. Its relativistic counterpart is the Maxwell-Jüttner distribution, given by

$$f(\vec{v})\,\mathrm{d}\vec{v} = \frac{1}{4\pi m^2 c k_{\mathrm{B}}T}K_2^{-1}\left(\frac{mc^2}{k_{\mathrm{B}}T}\right)\exp\left(\frac{\gamma mc^2}{k_{\mathrm{B}}T}\right)\mathrm{d}\vec{v}\,, \tag{1.2}$$

with $\gamma = \gamma(\vec{v})$ denoting the usual Lorentz factor, and K_2 being the modified Bessel function of the second kind.

From eq. 1.1 and eq. 1.2, it is possible to perform order-of-magnitude estimates for the number of particles with energies above a certain threshold. For instance, considering the peak of this distribution, the temperature required to get thermal particles with energies of $\sim 10^{20}$ eV, which is the ballpark for the most energetic ultra-high energy cosmic rays (UHECRs) ever recorded [1, 2], is $T \gtrsim 10^{24}$ K — far beyond the temperatures found in astrophysical environments. For comparison, the cores of some exploding start can reach temperatures of up to 10^{11} K, still far from the required 10^{19} K. *Therefore, there are no viable thermal mechanisms for producing high-energy particles.*

To produce high-energy particles, one must resort to non-thermal mechanisms. It is rea-

sonable to suppose that either these particles are produced by some higher-energy entity — the so-called *top-down* scenarios — or that they are accelerated from lower energies to higher energies — the *bottom-up* scenarios. Generally speaking, there is little room for top-down scenarios to be the sole responsible for the production of the highest-energy particles observed, given that this class of models often produce copious amounts of photons and neutrinos that are not detected [3–5]. Therefore, bottom-up mechanisms should dominate most (if not all) of the high-energy cosmic particle production. They are essentially based on the acceleration of particles in astrophysical environments, taking particles with initial energies E_i to a final energy $E_f > E_i$:

$$\frac{\Delta E}{E} \equiv \frac{E_f - E_i}{E_i} \, . \tag{1.3}$$

In bottom-up scenarios, particles start with relatively low energies and are boosted to higher energies through various astrophysical processes. Two key mechanisms underpin this paradigm:

- **electromagnetic acceleration:** particles are accelerated by electromagnetic fields in astrophysical environments;
- **gravitational acceleration:** acceleration is due to gravitational effects alone.

Electromagnetic acceleration is the standard and most widely accepted class of mechanisms. It is described in §1.1. The more unorthodox class of gravitational acceleration is discussed in §1.2.

1.1 Electromagnetic acceleration

1.1.1 Fermi acceleration: second order

This mechanism was originally proposed by Enrico Fermi in 1949 [6] to explain the acceleration of cosmic rays in the interstellar medium. It is based on the idea that particles can gain energy by bouncing off moving magnetic scattering centres. The process is schematically represented in fig. 1.1.

The process can be described as follows. Consider a particle of charge q and mass m moving with initial velocity $\vec{v}_i \equiv \beta_i c$. The particle crosses a magnetised region of space where the magnetic field is moving with velocity $\vec{V}$. This turbulent "cloud" can be intuitively thought of as a collection of magnetic scattering centres, off which charged particles can scatter, ultimately leading to an energy gain.

1.1.1.1 Energy gain

The energy gain of *one* "interaction" of the charged particle with the magnetic scattering centres is given byeq. 1.3. The information available, measured in the lab frame, is: the velocity of the magnetic scattering centres ($\vec{V}$); the energy (E_i) of the particle initially; the initial momentum ($\vec{p}_i$) of the particle; the angle the momentum vector forms with the moving scattering centres (θ_i). Suppose the final energy, as measured in the lab frame is E_f and
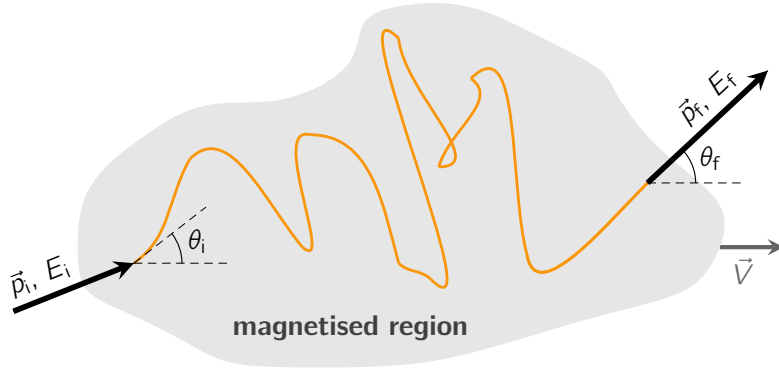
Figure 1.1: Schematic representation of the second-order Fermi acceleration process. A magnetised region moving with velocity $\vec{V}$, shown in grey, is crossed by a charged particle, whose trajectory is represented by the coloured lines. The particle is "scattered" by magnetic scattering centres of sorts, ultimately gaining energy.

the final momentum is $\vec{p}_f$, forming an angle θ_f with $\vec{V}$. The problem is that neither the final momentum nor the final energy are known. In fact, that is the whole point of studying the acceleration mechanism: to know how much energy the particle gains. Considering an ensemble of particles, the problem becomes solvable if one additional hypothesis is considered: that the final scattering angles *in the cloud rest frame* are isotropically distributed. This is a reasonable assumption, considering that the medium is turbulent and many scatterings are expected to occur. The problem would be solvable if some additional information about the final. Therefore, both frames have to be considered in the calculation, the lab frame, in which both the particle and the cloud are moving (fig. 1.1), and the rest frame of the cloud. The quantities in the latter frame are indicated by a prime.

Let $\gamma \equiv 1/\sqrt{1-\beta^2}$ designate the Lorentz factor of the cloud, with $\beta \equiv V/c$. The energy of the incoming particle in the cloud rest frame is given by

$$E_i' = \gamma\left(E_i - \vec{V} \cdot \vec{p}_i\right) \tag{1.4}$$

In second order Fermi acceleration, it is assumed that the velocity of the magnetic scattering centres is much smaller than the speed of light ($V \ll c$). Moreover, the speed at which the particle is moving (v) is also presumed to be relativistic, such that $E_i \approx p_i c$. This is a reasonable assumption, since the magnetic scattering centres are expected to be moving with velocities of the order of the Alfvén speed, which is typically much smaller than the speed of light. Therefore, eq. 1.4 can be recast into a more convenient form and solved for the initial energy in the lab frame:

$$E_i = \frac{E_i'}{\gamma\left(1 - \beta \cos\theta_i\right)} \,. \tag{1.5}$$

Similarly, the energy of the outgoing particle in the lab frame is related to the energy

measured in the cloud rest frame through the following expression:

$$E_f = \gamma E_f'\left(1 + \beta \cos\theta_f'\right). \tag{1.6}$$

Therefore, the energy gain of the particle in a single interaction is given by

$$\frac{\Delta E}{E} = \frac{E_f - E_i}{E_i} = \frac{E_f}{E_i} - 1 = \frac{\gamma E_f'\left(1 + \beta \cos\theta_f'\right)}{\dfrac{E_i'}{\gamma\left(1 - \beta \cos\theta_i\right)}} - 1. \tag{1.7}$$

At this stage, an additional consideration ought to be made. The energy of the particle in the cloud frame is conserved, such that $E_i' = E_f'$. This implies that the energy gain for one scattering can be written as

$$\boxed{\frac{\Delta E}{E} = \gamma^2\left(1 - \beta \cos\theta_i\right)\left(1 + \beta \cos\theta_f'\right) - 1.} \tag{1.8}$$

Now that the energy gain of a single interaction is known, the next step is to calculate the average energy gain of the particle after several interactions. This is done by averaging the energy gain over all possible incoming angles (θ_i) and all possible final angles (θ_f), assuming that the final angle is isotropically distributed in the cloud rest frame, i.e., $\langle\nu\rangle = 0$, where $\nu \equiv \cos\theta_f'$. This condition is equivalent to writing the probability distribution function

$$\mathrm{d}w_\nu \propto \mathrm{d}\Omega_\nu, \tag{1.9}$$

where $\mathrm{d}\Omega$ refers to the solid angle element corresponding to a zenith angle $\theta_f = \arccos\nu$. The initial scattering angle (θ_i), on the other hand, is not isotropically distributed, but rather follows a different type of distribution that favours head-on collisions over grazing ones. Let $\mu \equiv \cos\theta_i$. Then this distribution can be written as

$$\mathrm{d}w_\mu \propto \left(1 - \beta\mu\right)\mathrm{d}\Omega_\nu. \tag{1.10}$$

If many scatterings occurred within the cloud, the initial and final angles are completely uncorrelated[1], such that the joint probability distribution function can be written from eq. **??** and eq. **??** as

$$\frac{\mathrm{d}^2 w}{\mathrm{d}\Omega_\mu\,\mathrm{d}\Omega_\nu} = A\left(1 - \beta\mu\right), \tag{1.11}$$

where A is a normalisation constant.

The final step now is to average the individual scatterings, whose energy gains are given by eq. 1.8, considering the joint probability distribution function. This is done by integrating over all possible initial and final angles, weighted by the probability distribution functions (eq. 1.11):

---

[1]This condition is equivalent to saying that the Jacobian is one, which ensures that the two-dimensional function is separable.

$$\left\langle \frac{\Delta E}{E} \right\rangle = \frac{\iint \frac{\Delta E}{E} \frac{\mathrm{d}^2 w}{\mathrm{d}\Omega_\mu \, \mathrm{d}\Omega_\nu} \, \mathrm{d}\Omega_\mu \, \mathrm{d}\Omega_\nu}{\iint \frac{\mathrm{d}^2 w}{\mathrm{d}\Omega_\mu \, \mathrm{d}\Omega_\nu} \, \mathrm{d}\Omega_\mu \, \mathrm{d}\Omega_\nu} \,. \tag{1.12}$$

Since $\mathrm{d}\Omega = \sin\theta \mathrm{d}\theta \mathrm{d}\varphi$, where θ and φ refer to the zenith and azimuthal angles, respectively, the integrals in eq. 1.12 in the ranges $-1 \leq \mu \leq 1$ and $-1 \leq \nu \leq 1$ yield

$$\left\langle \frac{\Delta E}{E} \right\rangle = \frac{4\beta^2}{3(1 - \beta^2)} \,. \tag{1.13}$$

Since $V \ll c$, it follows that $\beta^2 \ll 1$, thus implying[2]

$$\boxed{\left\langle \frac{\Delta E}{E} \right\rangle \simeq \frac{4}{3}\beta^2 \,.} \tag{1.14}$$

Eq. 1.14 is second-order in β, hence the name of the mechanism. This is clearly not an efficient process, since the average gain per scattering is rather low. However, the key point is that the process is cumulative, leading to a net energy gain. On the other hand, it is stochastic, which reduces its efficiency.

The principle underlying this mechanism is the scattering off magnetic centres. But magnetic fields do no work. Therefore, "who" is actually doing the acceleration? The answer is: the electric field. An electric field is simply a magnetic field viewed from another frame. Therefore, it is reasonable to suppose that an alternative approach to the mechanism, using electric fields, could lead to the same results. This approach is discussed in §1.1.1.2.

1.1.1.2 Energy gain: derivation from electric fields

1.1.1.3 Spectrum of accelerated particles

Suppose the charged particle from 1.1 remains trapped in the accelerating region for a time τ_{esc}, and assume there are no energy losses, only energy gain. Let $N(E)$ be the number of particles with energies between E and $E + \mathrm{d}E$. Energy conservation implies

$$\frac{\mathrm{d}}{\mathrm{d}E}\left[\frac{\mathrm{d}E}{\mathrm{d}t}N(E)\right] = -\frac{N(E)}{\tau_{\mathrm{esc}}} \,. \tag{1.15}$$

Since energy is gained and the process is repeated several times, until the particle escapes, a reasonable ansatz that captures this type of behaviour is

$$\frac{\mathrm{d}E}{\mathrm{d}t} = \frac{E}{\tau_{\mathrm{acc}}} \,, \tag{1.16}$$

---

[2]This equation differs by a factor of 2 with respect to some references, such as the classic textbook by Longair [7]. The reason for this is that here the average is done over all possible angles, whereas in the other case the derivation assumes a type of "reflection" off the magnetic scattering centres.

wherein τ_{acc} is the acceleration time scale. As a consequence, the equation can be rewritten as

$$\frac{\mathrm{d}N(E)}{\mathrm{d}E} = -\underbrace{\left(1 + \frac{\tau_{\text{acc}}}{\tau_{\text{esc}}}\right)}_{\equiv\alpha} \frac{N(E)}{E} \, . \tag{1.17}$$

Therefore, the spectrum of stochastically Fermi-accelerated particles is given by

$$N(E) = N_0 E^{-\alpha+1} \tag{1.18}$$

or, in a more convenient spectral form,

$$\boxed{\frac{\mathrm{d}N}{\mathrm{d}E} \propto E^{-\alpha} \, .} \tag{1.19}$$

Note that eq. 1.15, used to derive the spectrum of eq. 1.19, is evidently simplified. It can be identified as a diffusion type of equation in the steady state, with no diffusion and no interactions. A proper treatment of the problem would involve solving the complete and more realistic version of this equation. Realistically, $\tau_{\text{acc}} = \tau_{\text{acc}}(E)$ and $\tau_{\text{esc}} = \tau_{\text{esc}}(E)$, due to, e.g., momentum diffusion (see §2.2.3 for details). This can result in modifications of the spectrum at the highest energies, leading to features such as broken power laws or smooth cutoffs.

1.1.2 Fermi acceleration: first order

First-order Fermi acceleration, commonly known as diffusive shock acceleration (DSA), is a mechanism that is particularly relevant in the context of astrophysical shocks. It addresses the major limitations of the second-order mechanism — the geometry — which reduces the efficiency of the acceleration. *If only there were more head-on "collisions", the energy gain would be higher...* Remarkably, this is actually realised in astrophysical environments in various types of shocks, described in more detail in §1.1.2.1.

1.1.2.1 Shocks

A shock is a discontinuity in the flow of something (like a fluid or a plasma), in which there are abrupt changes is some physical properties before and after it. These properties can be, for example, density, temperature, velocity, and sometimes magnetic field. In astrophysics, shocks play a fundamental role in a wide variety of phenomena, including the acceleration of cosmic rays, the heating of the interstellar medium, and the formation of stars and galaxies.

Astrophysical shocks can be collisional or collisionless depending on whether particle collisions or collective electromagnetic fields dominate the shock formation process. In much of the diffuse astrophysical plasma, Coulomb collisions are relatively infrequent, and collisionless shocks (mediated by plasma instabilities and electromagnetic fields) are common. Nevertheless, many properties of collisionless shocks can be understood using classical fluid models (e.g., magnetohydrodynamics), supplemented with additional plasma-physics considerations.
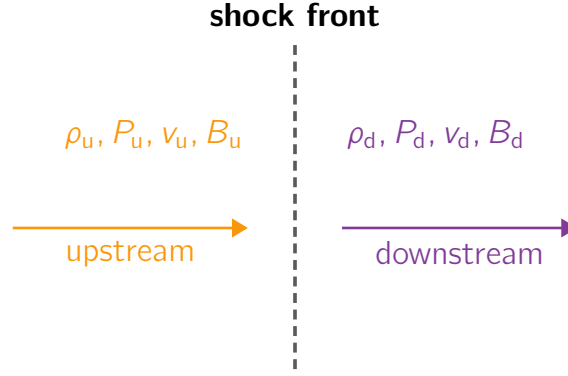
shock front

Figure 1.2: A schematic representation of a shock. The front of the shock, assumed to be at rest, is located at $x = 0$. The upstream region is labelled 'u' and the downstream region is labelled 'd'. Relevant quantities are: density (ρ), pressure (P), temperature (U), velocity (v), and magnetic field (B).

The *Rankine-Hugoniot conditions* (a.k.a. **jump conditions**) provides the foundations for the study of shocks. They describe how some physical properties change before and after the shock. They are derived from the integration of conservation laws before and after the shock.

For starters, consider the simple case of a shock at $x = 0$, stationary in this reference frame. Consider a steady, one-dimensional shock. The pre-shock (or upstream) region is labelled 'u' and the post-shock (or downstream) region is referred to by the subscript 'd'. The Rankine-Hugoniot jump conditions for a perfect (non-magnetised) fluid are:

$$\rho_u v_u = \rho_d v_d, \tag{1.20}$$

$$\rho_u v_u^2 + P_u = \rho_d v_d^2 + P_d, \tag{1.21}$$

$$\frac{1}{2}\rho_u v_u^2 + \frac{\gamma_c}{\gamma_c - 1}P_u = \frac{1}{2}\rho_d v_d^2 + \frac{\gamma_c}{\gamma_c - 1}P_d. \tag{1.22}$$

Here γ_c represents the ratio between the specific heats of the gas (do not confuse it with the Lorentz factor), $\gamma_c = c_p/c_v$, where c_p and c_v are the specific heats at constant pressure and volume, respectively. Three conservation laws are used in the derivation of these equations: mass flux conservation, momentum flux conservation, and energy flux conservation. They are derived by integrating the conservation laws across the shock interface.

The fluid is compressed and heated after crossing the shock front, such that the downstream region is denser ($\rho_u < \rho_u$) than the upstream, and both its temperature and pressure also exceed those in the downstream region ($P_d > P_u$ and $T_d > T_u$). For a non-relativistic monoatomic gas, $\gamma_c = 5/3$ and the Rankine-Hugoniot conditions lead to the strong shock jump conditions:

$$\rho_d = 4\rho_u, \tag{1.23}$$

$$v_u = 4v_d. \tag{1.24}$$

1.1.2.2 Energy gain

The principle of the mechanism is the same as in the second-order case, such that eq. 1.8 still holds. However, there is a very important difference with respect to the previous case: the geometry. While eq. 1.12 is still valid, since the first-order mechanism deals with shocks, the weighting functions used for averaging (eq. 1.11) has to be corrected.

The first-order mechanism is more efficient than the second, since the averaging procedure naturally favours head-on collisions. The idea is that particles can gain energy by crossing a shock front multiple times. These crossings, illustrated in fig. **??**, are responsible for the acceleration of particles to high energies. If the shock front is very large, such that its curvature can be neglected, the angular dependence for one cycle of scattering, which consists in upstream→downstream→upstream (this will henceforth be called a *cycle*), will depend only on the angle of the particle with respect to the shock. Therefore, an expression equivalent to 1.11 can be written:

$$\mathrm{d}w \propto \mu\nu\,\mathrm{d}\Omega_\mu\mathrm{d}\Omega_\nu\,, \tag{1.25}$$

which when plugged into eq. 1.12 yields

Particles crossing the shock from upstream to downstream are constrained to the range $0 \leq \mu \leq -1$, since they are antiparallel to the shock motion. Particles crossing the shock from downstream to upstream, on the other hand, are parallel to the shock motion, and are therefore in the range $0 \leq \nu \leq 1$. Consequently, the integral in eq. 1.12 can be written as

$$\left\langle \frac{\Delta E}{E} \right\rangle = \frac{4\beta + \beta^2}{3(\beta^2 - 1)}\,. \tag{1.26}$$

Since $0 \leq \beta \leq 1$, this expression can be approximated to the terms first-order in β, yielding

$$\boxed{\left\langle \frac{\Delta E}{E} \right\rangle \simeq \frac{4}{3}\beta\,.} \tag{1.27}$$

As in the second-order case, the mechanism is called first-order because it depends on the first power of β.

1.1.2.3 Spectrum of accelerated particles

This mechanism is essentially a pinball machine, where particles bounce back and forth across the shock front, gaining energy at each crossing. The energy gain per crossing is given by eq. 1.8, and the average energy gain is given by eq. 1.27.

Suppose initially N_0 particles were injected with energy E_0, each having a probability $\mathcal{P}_{\mathrm{esc}}$ of escaping after the acceleration. After k cycles, crossing the shock front down and upstream again, the charged particle will acquire an energy

$$E_k = E_0 \left(1 + \frac{\Delta E}{E}\right)^k \equiv E_0 \xi^k\,. \tag{1.28}$$

The probability that the particle will escape at any given cycle is $\mathcal{P}_{\text{esc}}$, such that after the same k cycles the total number of particles that remain trapped in the accelerating region is

$$N = N_0 \left(1 + \mathcal{P}_{\text{esc}}\right)^k . \tag{1.29}$$

Therefore, the spectrum of accelerated particles is given by

$$\frac{\mathrm{d}N}{\mathrm{d}E} \propto E^{-\alpha} , \tag{1.30}$$

where

$$\alpha \equiv 1 - \frac{\ln \mathcal{P}_{\text{esc}}}{\ln \xi} . \tag{1.31}$$

This is the same power-law form as in the second-order case, but with a possibly different value of α.

The escape probability can be estimated following Bell [8]. Assuming an isotropic distribution of particles with number density n, the average flux of particles crossing a surface is $\frac{1}{4} n \tilde{\beta} c$, for a characteristic velocity of the particles $\tilde{\beta}$. This flux does not change for upstream $\rightarrow$ downstream or downstream $\rightarrow$ upstream.

When the particles are downstream of the shock, they can be trapped in the plasma flow moving away from the shock with velocity $\vec{u}$. In In other words, in the downstream rest frame, the particle distribution remains isotropic, so the number of particles swept away from the shock front per unit area per unit time is also $\frac{1}{4} n u$. This can be interpreted as the outgoing particle flux that is lost from the acceleration zone, since those particles no longer cross to the upstream side.

The ratio of this advected flux ($\frac{1}{4} n u$) to the incoming flux ($\frac{1}{4} n \tilde{\beta} c$) indicates the fraction of particles that *do not* return to the shock within one single cycle:

$$\frac{\frac{1}{4} n u}{\frac{1}{4} n \tilde{\beta} c} = \frac{u}{\tilde{\beta} c} . \tag{1.32}$$

This fraction is the escape probability, $\mathcal{P}_{\text{esc}}$:

$$\mathcal{P}_{\text{esc}} = 1 - \frac{u}{\tilde{\beta} c} . \tag{1.33}$$

For non-relativistic shocks, considering that the particle velocity is relativistic ($\tilde{\beta} \rightarrow 1$), this implies that $\alpha = 2$.

Moreover, energy losses in the medium could play an important role in slowing down the acceleration. And on top of that, one has to consider that the shock is magnetised, such that the particles will diffuse differently in the upstream and downstream of the shock.

The early theory of DSA dates back to the 1970s. Krymskii [9] was arguably the first to formally identify the idea that the scattering of charged particles off an expanding shock such as a supernova remnant would lead to first-order energy gain. Axford, Leer, and Skadron [10]

stressed the importance of pitch-angle scattering by magnetic turbulence (see §2.1.2) in the acceleration process. This is essentially the current notion of resonant scattering.

Blandford and Ostriker [11] and Bell [12] independently developed the theory of DSA in the context of supernova remnants. In particular, Blandford and Ostriker [11] linked the theory of DSA with observations, stressing an observational consequence of DSA: the radio emission of synchrotron radiation from accelerated electrons in supernova remnants (SNRs), as shown in fig. 1.3. Drury [13] and subsequently many other authors formalised the theory of DSA and cast it in a Fokker-Planck framework. This allowed for a more detailed treatment of the acceleration process, including the effects of energy losses and magnetic turbulence. Around this time, DSA became the dominant paradigm for the acceleration of charged particles in astrophysical environments.
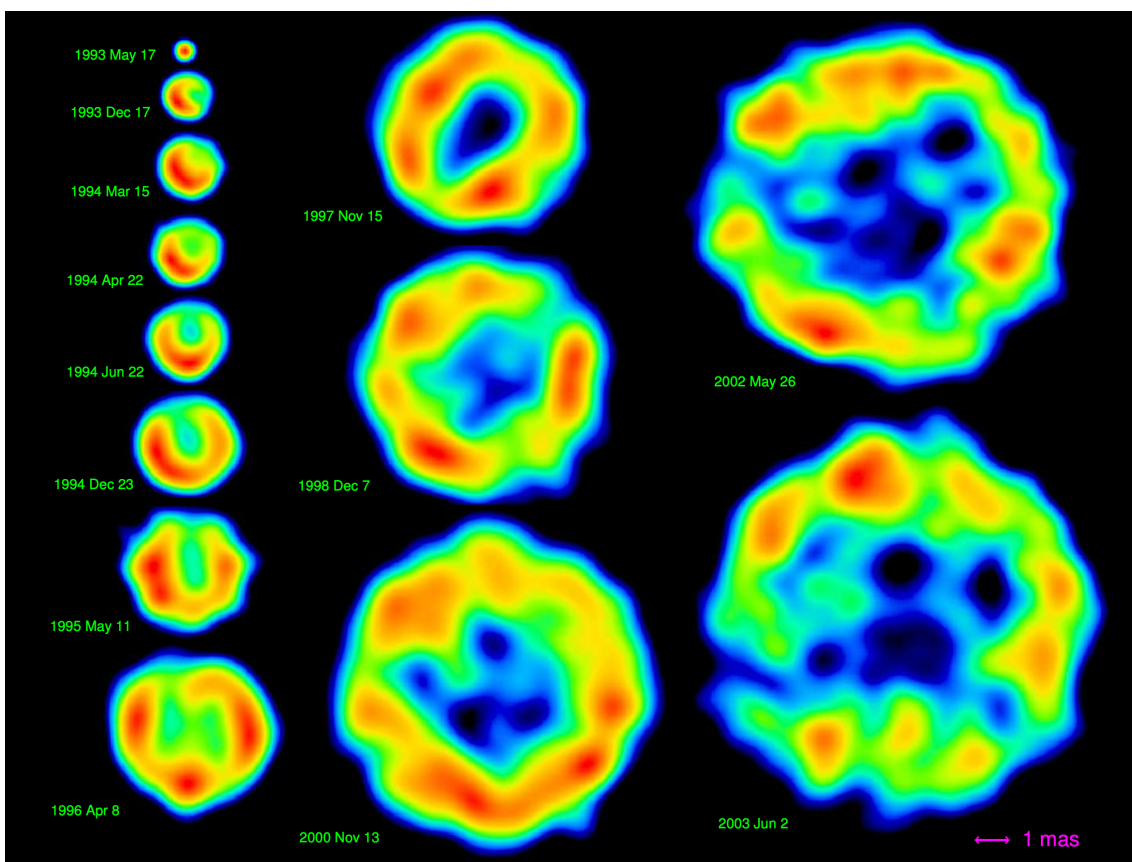
Figure 1.3: SN1993J at different epochs. The colour scale indicates the intensity of radio emission, from lower (colder shades) to higher values (warmer colours). The radio emission is attributed to synchrotron radiation from accelerated electrons in the shock front. This also explains why most of the signal is not at the centre. The shock is estimated to be moving with a velocity of $\simeq 20000$ km/s. Figure taken from Bietenholz [14].

The theory has since been extended to include the effects of the feedback of the accelerated particles onto the environment, which leads to non-linear effects such as magnetic-field amplification. Nevertheless, the basic idea of DSA remains the same: particles gain energy by crossing a shock front multiple times, and the spectrum of accelerated particles is a power

law.

1.1.3 Unipolar induction

1.2 Gravitational acceleration

The general principle of gravitational acceleration is that particles can gain energy by falling into a gravitational potential well. In particular, there are orbits with negative potential energy, which can be exploited to accelerate particles. This is the underlying principle of a class of mechanisms called Penrose processes [15]

The principle is usually applied to rotating black holes. The general idea is simple. First, a particle falls into the ergosphere of a black hole (BH). Then, the particle splits into two fragments, one of which follows an orbit of negative potential energy. This allows the other particle to escape the ergosphere with a higher energy than the original particle.

The same process can occur if two particles collide inside the ergosphere — the collisional Penrose process.

1.3 Conditions for acceleration

A cosmic accelerator must satisfy a few conditions to be able to produce high-energy particles. There are at least three necessary conditions that must be met for particles to be accelerated to high energies:

- energy gain;
- confinement;
- power.

The first is a general criterion that must be satisfied regardless of how particles are accelerated is that the rate at which the particle gains energy must exceed the energy loss rate, which is to say

$$\left.\frac{\mathrm{d}E}{\mathrm{d}t}\right|_{\mathrm{gain}} > \left.\frac{\mathrm{d}E}{\mathrm{d}t}\right|_{\mathrm{loss}}. \tag{1.34}$$

This obvious condition also determines the efficiency of the acceleration process and its time scale.

The other criteria are described in §1.3.1 and §1.3.2. Some authors (e.g. [16]) consider additional criteria. Nevertheless, the three mentioned here are necessary (but not sufficient) conditions.

1.3.1 The Hillas criterion

A geometrical criterion that constraints the electromagnetic acceleration of particles is the so-called Hillas criterion [17]. This necessary condition for acceleration relates the size of the region (R_{o}) to the Larmor radius of the particle (R_{L}). If the region is too small, particles will

escape before being accelerated. Therefore, the condition is $R_o \gtrsim R_L$:

$$R_o \gtrsim \frac{E}{|q|B_o} \, , \tag{1.35}$$

where E is the energy of the particle, and B_o the magnetic field strength in the region.

The maximum energy that can be attained by a charged particle is:

$$\boxed{E_{max} \simeq \frac{q}{e} \beta R_o B_o \, ,} \tag{1.36}$$

where $\beta \equiv v/c$ refers to the velocity of the particle.

This criterion is illustrated in fig. 1.4.
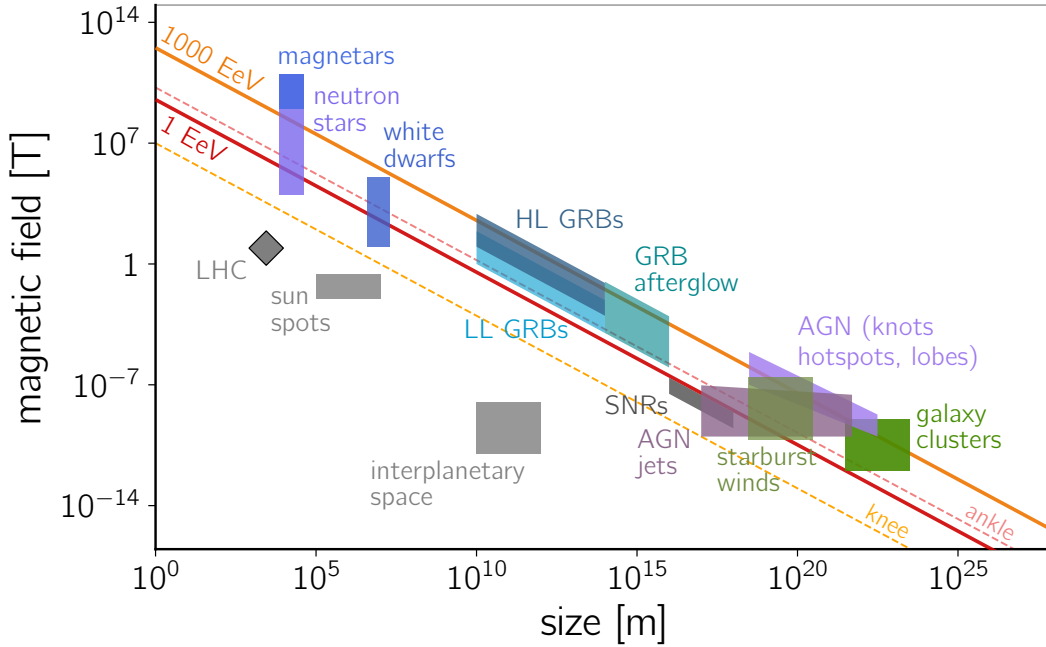
Figure 1.4: *The Hillas plot*, illustrating the parameter space of magnetic field strength (vertical axis) and confinement size of the region (horizontal axis). Above the lines which represent different reference energies, particles are no longer magnetically confined to the region, assuming Bohm diffusion. Figure taken from [18].

1.3.2 The Hillas-Lovelace condition

The third criterion is the Hillas-Lovelace condition, which is a generalisation of the Hillas criterion. It states the (rather obvious) fact that there must be enough power to accelerate particles to high energies. If this energy is magnetically-sourced, the resulting power constraint is [17, 19]:

$$L_{B,min} \gtrsim \beta c u_B R_o^2 \, , \tag{1.37}$$

with u_B denoting the magnetic energy density.

16

1.4 Exercises

1.1   Fermi acceleration is usually classified into two main categories: first-order and second-order acceleration.

(a) Explain the main differences between Fermi 1st order and Fermi 2nd order acceleration in terms of:

- physical mechanism;
- energy gain per interaction;
- the efficiency of the acceleration process.

(b) Why is 1st-order Fermi acceleration (shock acceleration) generally considered more efficient than the 2nd-order mechanism, in astrophysical contexts?

1.2   In 2nd-order Fermi acceleration, the energy gain per scattering is given by:

$$\frac{\Delta E}{E} \simeq \frac{4}{3}\beta^2 \,,$$

where $\beta = v/c$ is the velocity of the scattering centre in units of the speed of light. Suppose the magnetic field in the accelerating region has a coherence length of L_B, and assume that particles are moving at ultra-relativistic speeds.

Write down an expression for the number of scatterings (N_{scat}) required for a particle to reach an energy of E, starting from an initial energy of E_0.

1.3   In the Fermi 1st-order acceleration mechanism, particles are scattered back and forth across a shock front. Suppose a particle of energy E_0 is scattered k times by the shock front.

(a) Compute the energy of the particle after k scatterings.

(b) Let $\mathcal{P}_{\text{esc}}$ be the probability that a particle will escape the accelerating region after k scatterings. Show that the number of particles that remain trapped is given by

$$N = N_0 \left(1 + \mathcal{P}_{\text{esc}}\right)^k \,.$$

(c) Show that the spectrum of accelerated particles in this case forms a power-law distribution.

1.4   Consider a plasma of fully ionised hydrogen (i.e., a monatomic gas) with negligible internal thermal energy upstream of a shock. Make the oversimplification that the unshocked gas is cold and pressureless. Derive the strong shock jump conditions:

$$\rho_{\text{d}} = 4\rho_{\text{u}} \,,$$
$$v_{\text{u}} = 4v_{\text{d}} \,.$$

1.5   The maximum energy a particle can reach in Fermi acceleration is determined by confinement within the acceleration region. The Hillas criterion provides an estimate for this

maximal energy (E_{max}) that can be reached by a particle of charge q (with $q \neq 0$) in a given astrophysical environment.

(a) Derive the Hillas criterion for the maximum energy a particle can reach:

$$E_{\text{max}} \approx q B_{\text{o}} R_{\text{o}} \,,$$

where R_{o} is the size of the acceleration region, and B_{o} is the magnetic field strength. Explain each step behind the derivation.

(b) Suppose a hydrogen nucleus (or proton) can be accelerated up to an energy of 3 PeV by a given astrophysical object. What is the maximal energy a helium nucleus can reach in the same environment?

Transport of charged particles in magnetic fields

The equation of motion of a single particle of charge q and mass m travelling with velocity $\vec{v}$ subject to a magnetic field $\vec{B}$ can be obtained starting off with the Lorentz force equation:

$$\frac{\mathrm{d}\vec{p}}{\mathrm{d}t} = m\frac{\mathrm{d}\vec{v}}{\mathrm{d}t} = q\vec{v} \times \vec{B}(\vec{x}, t) + q\vec{E}(\vec{x}, t)\,. \tag{2.1}$$

where $\vec{p} = \gamma m \vec{v}$ is the momentum of the particle, and $\gamma = \left(1 - v^2/c^2\right)^{-1/2}$ refers to the Lorentz factor. Here $\vec{E}$ denotes the electric field. It is convenient to write equation 2.1 as

$$\frac{\mathrm{d}\vec{v}}{\mathrm{d}t} = \frac{q}{m}\,\vec{v} \times \vec{B}(\vec{x}, t) + \frac{q}{m}\vec{E}(\vec{x}, t)\,, \tag{2.2}$$

with c denoting the speed of light.

For starters, consider the case of homogeneous magnetic and electric fields: $|\vec{E}| = \vec{E}_0$ and $|\vec{B}| = \vec{B}_0$. Eq. 2.2 can be more easily solved by introducing the transformation

$$\vec{v}' = \vec{v} - \frac{1}{B^2}\vec{E} \times \vec{B}\,, \tag{2.3}$$

and by noting that $\vec{E} \cdot \vec{B} = 0$ is a relativistic invariant[1]. The term that contains $\vec{E} \times \vec{B}$ causes the motion of the particle in a direction perpendicular to both the electric and the magnetic fields. This is the **drift velocity**:

$$\vec{v}_d = \frac{\vec{E} \times \vec{B}}{B^2}\,. \tag{2.4}$$

Eq. 2.2 is then simply given by

$$\frac{\mathrm{d}\vec{v}'}{\mathrm{d}t} = \frac{q}{m}\,\vec{v}' \times \vec{B}\,. \tag{2.5}$$

This transformation can also be understood as a choice of a reference frame wherein the

---

[1]This statement is factually correct for a single particle moving in vacuum. There are systems in which $\vec{E} \cdot \vec{B} \neq 0$. These usually involve media and materials that are neither ideal conductors nor insulators.

electric field is null (frame $\mathcal{S}'$), instead of the original frame $\mathcal{S}$ in which it is non-zero.

> **Exercise.** Show that there is a frame ($\mathcal{S}'$) in which the electric field is zero. Does such a frame *always* exist? What happens to the drift velocity in this frame?

Having established the equivalence of the equations of motion 2.2 and 2.18, it is clear that much can be learned in an easier fashion if the frame $\mathcal{S}'$ is chosen, such that the electric field is neglected altogether. Therefore, in what follows, this will be taken into account. Nevertheless, to keep the notation concise, the prime symbols will be dropped for simplicity. This is completely equivalent to the case $\vec{E} = 0$. In fact, this is an appropriate choice because in many astrophysical environments like the ones of interest here (e.g., intergalactic medium, intracluster medium, etc), the pervading plasmas have high conductivity, such that there are no large-scale electric fields ($\vec{E} \approx 0$).

2.1 Transport of a single particle

2.1.1 Homogeneous magnetic field

For simplicity, take a coordinate system wherein the magnetic field is oriented along the z axis, i.e., $\vec{B} = B_0 \hat{z}$. The velocity component of $\vec{v}$ in the z direction is completely arbitrary (but constant) and irrelevant for propagation because of the vector product $\vec{v} \times \vec{B}$. Thus, the solution can be obtained by solving a system of two differential equations of first order in the velocity:

$$
\begin{cases}
\dfrac{\mathrm{d}v_x}{\mathrm{d}t} = \dfrac{q}{mc}B_0 v_y & \equiv \omega v_y \\[2mm]
\dfrac{\mathrm{d}v_y}{\mathrm{d}t} = -\dfrac{q}{mc}B_0 v_x & \equiv -\omega v_x \\[2mm]
\dfrac{\mathrm{d}v_z}{\mathrm{d}t} = 0 &
\end{cases}
\tag{2.6}
$$

To simplify the notation, the **gyrofrequency** $\omega \equiv |q|B_0/mc$ is defined. In addition, the parallel and the perpedincular components of the velocity with respect to the magnetic field are introduced: $\vec{v}_{\parallel}(t) \equiv v_z(t)\hat{z}$ and $\vec{v}_{\perp}(t) \equiv v_x(t)\hat{x} + v_y(t)\hat{y}$.

In general, $\vec{v}(t) = \vec{v}_{\parallel}(t) + \vec{v}_{\perp}(t)$, but in this particular case these quantities are all constant ($|\vec{v}_{\parallel} + \vec{v}_{\perp}| = |\vec{v}| = \text{constant}$). A useful concept that can be introduced at this stage is the **pitch angle**, ϕ_p, which links the parallel and perpendicular components of the velocity as follows:

$$
\tan \phi_p(t) = \frac{v_{\perp}(t)}{v_{\parallel}(t)} .
\tag{2.7}
$$

For a simple homogeneous magnetic field like $\vec{B} = B_0\hat{z}$, the pitch angle is constant. This follows from the fact that $\frac{\mathrm{d}v_{\parallel}}{\mathrm{d}t} = 0$ implies $\frac{\mathrm{d}v_{\perp}}{\mathrm{d}t} = 0$ at all times.

The solution of this system of differential equations is immediate:

$$v_x(t) = v_\perp \cos(\phi - \omega t)\,, \tag{2.8}$$

$$v_y(t) = v_\perp \sin(\phi - \omega t)\,, \tag{2.9}$$

$$v_z(t) = v_\parallel\,, \tag{2.10}$$

where ϕ is a constant indicating the initial phase of the system. To obtain the time-dependence of the coordinates, these equations should be integrated, yielding

$$x(t) = x(0) + \frac{v_\perp}{\omega} \sin\phi - \frac{v_\perp}{\omega} \sin(\phi - \omega t)\,, \tag{2.11}$$

$$y(t) = y(0) - \frac{v_\perp}{\omega} \cos\phi + \frac{v_\perp}{\omega} \cos(\phi - \omega t)\,, \tag{2.12}$$

$$z(t) = z(0) + v_\parallel t\,. \tag{2.13}$$

Note that

$$v_x^2(t) + v_y^2(t) = \text{constant}\,, \tag{2.14}$$

which is a circular motion in the xy plane around the point

$$(x_{\text{centre}}, y_{\text{centre}}) = \left(x(0) + \frac{v_\perp}{\omega} \sin\phi,\ y(0) - \frac{v_\perp}{\omega} \cos\phi \right)\,. \tag{2.15}$$

It is possible to identify a characteristic quantity with dimensions of length related to the gyrofrequency. This is the **Larmor radius** (or gyroradius), given by

$$R_L = \frac{v_\perp}{\omega}\,. \tag{2.16}$$

This general definition can be rewritten in a more convenient form in terms of the energy $E = \gamma m c^2$ of the particle:

$$\boxed{R_L = \frac{E}{|q|cB_0}\,.} \tag{2.17}$$

Note that this approximation is only valid for pitch angles that satisfy $\tan\phi_p \sim 0$.

2.1.2 Inhomogeneous magnetic field

Consider now a perturbation $\delta\vec{B}$ to the simple magnetic field from §2.1.1, which can be in an arbitrary direction. The total field now reads $\vec{B} = \vec{B}_0 + \delta\vec{B} = B_0\hat{z} + \delta\vec{B}$. This can now be plugged into the general equation of motion (eq. 2.1):

$$\frac{\mathrm{d}\vec{v}}{\mathrm{d}t} = \frac{qc^2}{E} \vec{v} \times \vec{B} = \frac{\omega}{B_0} \vec{v} \times \vec{B}_0 + \frac{\omega}{B_0} \vec{v} \times \delta\vec{B}\,. \tag{2.18}$$

The solution for first term on the right-hand side of the last equality is known (eq. 2.10 and eq. 2.13).

To obtain the full solution, one must first write down the system of differential equations:

$$\begin{cases} \dfrac{dv_x}{dt} = \omega_0 \left(v_y \dfrac{\delta B_z}{B_0} - v_z \dfrac{\delta B_y}{B_0} \right) + \omega_0 v_y\,, \\[2ex] \dfrac{dv_y}{dt} = \omega_0 \left(v_z \dfrac{\delta B_x}{B_0} - v_x \dfrac{\delta B_z}{B_0} \right) - \omega_0 v_x\,, \\[2ex] \dfrac{dv_z}{dt} = \omega_0 \left(v_x \dfrac{\delta B_y}{B_0} - v_y \dfrac{\delta B_x}{B_0} \right)\,, \end{cases} \tag{2.19}$$

where ω_0 is what was formerly ω, this is, the gyrofrequency corresponding to the unperturbed magnetic field. Note that each i-th component of the perturbations are assumed to vary slowly with time, such that $\frac{d\delta B_i}{dt} \sim 0$.

The differential equation 2.19 can be solved using variation of parameters. For simplicity, let $a_i(t)$ be the terms within parentheses times ω_0. The ansatz is the following:

$$v_x(t) = g_1(t)\cos\omega_0 t + g_2(t)\sin\omega_0 t\,, \tag{2.20}$$
$$v_y(t) = g_2(t)\cos\omega_0 t - g_1(t)\sin\omega_0 t\,, \tag{2.21}$$

where $g_1(t)$ and $g_2(t)$ are two functions to be determined. By inspection, it is possible to show that

$$g_1(t) = \int_0^t dt'\, \left[a_y(t')\cos\omega_0 t' - a_x(t')\sin\omega_0 t' \right]\,, \tag{2.22}$$

$$g_2(t) = \int_0^t dt'\, \left[a_y(t')\sin\omega_0 t' + a_x(t')\cos\omega_0 t' \right]\,. \tag{2.23}$$

After some tedious integrations (by parts), the velocities are obtained:

$$v_x(t) = v_x(0)\cos\omega_0 t + v_y(0)\sin\omega_0 t + \cos\omega_0 t \int_0^t dt'\, \left[a_y(t')\cos\omega_0 t' - a_x(t')\sin\omega_0 t' \right]$$
$$+ \sin\omega_0 t \int_0^t dt'\, \left[a_y(t')\sin\omega_0 t' + a_x(t')\cos\omega_0 t' \right]\,,$$

$$\tag{2.24}$$

and

$$v_y(t) = v_y(0)\cos\omega_0 t - v_x(0)\sin\omega_0 t + \cos\omega_0 t \int_0^t dt'\, \left[a_y(t')\sin\omega_0 t' + a_x(t')\cos\omega_0 t' \right]$$
$$- \sin\omega_0 t \int_0^t dt'\, \left[a_y(t')\cos\omega_0 t' - a_x(t')\sin\omega_0 t' \right]\,.$$

$$\tag{2.25}$$

The guiding centre follows the magnetic-field lines. The motion is a superposition of two components, one that rotates in the xy plane, and another that moves stochastically as determined by the perturbing field. A better understanding of this motion can be grasped by considering an arbitrary instant in time (t) and integrating the velocities over one period:

$$u_i(t) = \frac{1}{T} \int_t^{t+T} dt' \, v_i(t') \,, \tag{2.26}$$

where $T = 2\pi/\omega_0$ is the period of the particle. It follows then that

$$\begin{aligned}
u_x(t) &\approx \frac{1}{\omega_0} a_x(t) = v_z \frac{\delta B_x}{B_0} - v_x \frac{\delta B_z}{B_0} \,, \\
u_y(t) &\approx \frac{-1}{\omega_0} a_y(t) = v_z \frac{\delta B_y}{B_0} - v_y \frac{\delta B_z}{B_0} \,, \\
u_z(t) &\equiv v_z(t) \,.
\end{aligned} \tag{2.27}$$

To solve eq. 2.27, it is necessary to know the perturbation $\delta \vec{B}$. This is a difficult task, as it is not possible to know the exact form. However, it is possible to obtain the average motion of a collection of particles, as will be shown in the next section.

2.2 Transport of an ensemble particles in magnetic fields

In §2.1.1 the equation of motion for a particle in a homogeneous magnetic field were derived. Now In §2.1.2 a perturbation was added to the homogenous field to obtain a more general set of equations of motion. *What happens if the magnetic field is inhomogeneous?* To answer this question, it is useful to understand analogous processes like Brownian motion. In essence, the underlying mathematical formalism involves calculating **random walks**.

2.2.1 Random walks

In one dimension a random walker can move in either direction, left or right. In the isotropic case, both probabilities are the same, i.e., $\mathcal{P}(\text{left}) = \mathcal{P}(\text{right})$. Suppose a displacement of n steps of length λ, where λ is much smaller than the length scale of the system. The position of the particle in this case is

$$x(n) = \sum_{i=1}^{n} s_i \,, \tag{2.28}$$

where $s_i = \pm\lambda$, which means that the walker can move either left or right. The average displacement is

$$\langle x(n) \rangle = \left\langle \sum_{i=1}^{n} s_i \right\rangle \approx 0 \,. \tag{2.29}$$

The mean square is

$$\langle x^2(n) \rangle = \left\langle \sum_{i=1}^{n} s_i^2 \right\rangle = \lambda^2 n \, . \tag{2.30}$$

After n steps, the walker will have displaced k steps, where $k = n_l - n_r$ is the difference between the number of steps to the left (n_l) and the number of steps to the right (n_r), with $n = n_l + n_r$. The probability of finding any given value of k for a fixed n is

$$\mathscr{P}(k) = \frac{\text{number of } (n_l, n_r) \text{ arrangements}}{\text{total number of arrangements}} \, .$$

This yields:

$$\mathscr{P}(k) = \frac{\frac{n!}{n_r! n_l!}}{2^n} = \frac{n!}{2^n \left(\frac{n+k}{2}\right)! \left(\frac{n-k}{2}\right)!} \, . \tag{2.31}$$

Using Stirling's approximation ($\log(y!) = y \ln y - y$) the probability can be rewritten as

$$\ln \mathscr{P}(k) = n \ln n - \frac{1}{2} \left[(n+k) \ln(n+k) + (n-k) \ln(n-k) \right] \approx -\frac{k^2}{2n} \, , \tag{2.32}$$

which leads to

$$\mathscr{P}(k) = \exp\left(-\frac{k^2}{2n}\right) \, . \tag{2.33}$$

To obtain the results for the continuous case, recall that $x = k\lambda$. Therefore, replacing k in eq. 2.33, the probability becomes

$$\mathscr{P}(x) \propto \exp\left(-\frac{x^2}{2n\lambda^2}\right) \, . \tag{2.34}$$

The proportionality symbol is justified because there is no assurance that the distribution is an actual probability distribution function, which ought to be normalised to 1. A simple integration then gives the (normalised) probability distribution function for an isotropic random walk with characteristic length of λ after n steps:

$$\mathscr{P}(x) = \frac{1}{\sqrt{2\pi n\lambda^2}} \exp\left(-\frac{x^2}{2n\lambda^2}\right) \, . \tag{2.35}$$

To generalise the result from eq. 2.35 to three dimensions, note that the coordinates x, y, and z are completely independent, such that the probability for the 3D case is simply the product $\mathscr{P}(x)\mathscr{P}(y)\mathscr{P}(z)$:

$$\mathscr{P}(x, y, z) = \frac{1}{(2\pi n\lambda^2)^{\frac{3}{2}}} \exp\left(-\frac{x^2 + y^2 + z^2}{2n\lambda^2}\right) \, . \tag{2.36}$$

Assuming spherical symmetry, this becomes:

$$\mathcal{P}(r) = \frac{4\pi r^2}{(2\pi n\lambda^2)^{\frac{3}{2}}} \exp\left(-\frac{r^2}{2n\lambda^2}\right).$$ (2.37)

Physically, what is being modelled is the motion of a particle in an inhomogenous magnetic field, which can be viewed as a collection of regions in space (domains) wherein the field is approximately homogeneous. Each time a charged particle crosses one of these domains it will change directions, in a way similar to what a random walker does. For this reason, it is useful to quantify how often a particle crosses (or loosely speaking, "collides with") these regions. After a time t, the number n of interactions between the particle and the magnetic domains is $n = \Gamma t$, where Γ denotes the rate at which these interactions occur. Plugging this into eq. 2.37 results in

$$\mathcal{P}(r) = \frac{4\pi r^2}{(2\pi n\lambda^2)^{\frac{3}{2}}} \exp\left(-\frac{r^2}{2\Gamma\lambda^2 t}\right).$$ (2.38)

An essential concept can now be introduced relating the motion of a particle with the frequency of interactions with the magnetic domains. The **diffusion coefficient** is defined as

$$D \equiv \frac{1}{2}\Gamma\lambda^2.$$ (2.39)

Now the probability from eq. 2.38 becomes

$$\boxed{\mathcal{P}(r) = \frac{4\pi r^2}{(4\pi D t)^{\frac{3}{2}}} \exp\left(-\frac{r^2}{4Dt}\right).}$$ (2.40)

The mean displacement can be shown to be null:

$$\langle r \rangle = \int_0^\infty \mathcal{P}(r) r \, dr = 0.$$ (2.41)

Similarly, the mean of the squared displacements can be calculated:

$$\langle r^2 \rangle = \int_0^\infty \mathcal{P}(r) r^2 \, dr = 6Dt.$$ (2.42)

Note that for each individual coordinate x, y, and z, the corresponding mean squared displacement is, on average:

$$\langle \Delta x^2 \rangle = \langle \Delta y^2 \rangle = \langle \Delta z^2 \rangle = \frac{1}{3}\langle r^2 \rangle.$$

This is true in case of isotropy, which guarantees that all coordinates are in equal footing, and in case of homogeneity, which ensures that $x(t) \rightarrow x(t) - x(0) \equiv \Delta x(t)$ (and similarly for y and z).

An important result about diffusion is delivered by eq. 2.42: $\sqrt{\langle r^2 \rangle} \propto \sqrt{t}$. If more realistic scenarios were considered, the general expression

$$\langle r^2 \rangle \propto t^\chi \tag{2.43}$$

would be obtained. Here the parameter χ determines the type of propagation. In this derivation using random walks the process was assumed to be Markovian and $\chi = 1$. For a homogeneous magnetic field (§2.1.1) or a perturbed field (§2.1.2), the regime of propagation is ballistic, with $\chi \geq 2$. This will become more clear when studying the propagation of an ensemble of particles. The other regimes of propagation are sub-diffusion ($0 < \chi < 1$) and superdiffusion ($1 < \chi < 2$).

This simple derivation of the diffusion of how a single particle diffuses in an inhomogeneous magnetic fields is instructive to understand some fundamental concepts, the diffusion coefficient being the most important of them. It encompasses the notion of coherence length through the size of the contiguous magnetic domain (λ), and the rate at which particles meet these domains (Γ) along the particle's trajectory, which is directly related to its velocity and Larmor radius. Naturally, this is simply a toy model for diffusion and the derivation is not rigorous, in addition to containing many simplifying assumptions mentioned throughout the text. For instance, firstly, diffusion can be anisotropic. Secondly, the magnetic domains might not be a good description for what happens in reality, their sizes may vary, and there might be correlations between them. Finally, this whole treatment was applied to a single particle, which is actually meaningless, given the statistical nature of the problem. It is, thus, important to realise that the perturbation is stochastic. So it is advantageous to work with an *ensemble* of particles, collectively, to understand the statistical properties of their propagation.

In §2.1.2 a perturbation was added to the magnetic field, and a set of equations (eq. 2.19) was obtained, but it was not directly solved because $\delta\vec{B}$ may be a function of position ($\vec{x}$) and time (t). They do, however, serve as bases for the subsequent discussions. In particular, the relationship between the mean squared displacements ($\langle \Delta x^2 \rangle$, $\langle \Delta y^2 \rangle$, and $\langle \Delta z^2 \rangle$; see eq. 2.42) and time through the diffusion coefficient will be used henceforth.

At this stage, a new concept comes in handy: the **running diffusion coefficient**, defined as:

$$d_{xx}(t) = \frac{1}{2}\frac{\mathrm{d}}{\mathrm{d}t}\left\langle (\Delta x(t))^2 \right\rangle . \tag{2.44}$$

Here the coordinate 'x' is simply a placeholder for all cartesian coordinates. It is "running" because it is a function of time. Another definition is also found in the literature, and here it will be denoted by D_{xx} to avoid confusion:

$$D_{xx}(t) = \frac{\left\langle (\Delta x(t))^2 \right\rangle}{2\Delta t} . \tag{2.45}$$

Taking the limit of infinite time, the diffusion coefficiente κ_{xx} – which is a constant –

corresponding to the running diffusion coefficient (d_{xx}) is obtained:

$$\kappa_{xx} = \lim_{t \to \infty} d_{xx}(t) . \tag{2.46}$$

Nevertheless, it should be noted that this quantity is only mathematically defined, as in reality time cannot be infinitely large. It suffices to employ d_{xx} to describe the system whenever $t \gg t_d$, i.e., when diffusive behaviour was reached after a time scale t_d.

These considerations show the importance of an *statistical* treatment of the relevant quantities, in particular the spatial coordinates. A useful mathematical toolkit to assist with these calculations is the Taylor-Green-Kubo (TGK) approach [20–22].

2.2.2 The Fokker-Planck equation

The Fokker-Planck equation was first introduced by Fokker [23] and Planck [24] in the context of statistical mechanics, and later re-derived by Kolmogorov [25]. It was motivated by the need to describe the transport of an ensemble of particles subject to drag and stochastic forces, in particular the changes in the probability density functions of the particle velocity. It can be understood as a phase-space equation that describes (statistically) the spatio-temporal evolution of a collection of particles. It is calculated in the phase space, including, therefore, spatial coordinates $(\vec{x})$, time (t), and momentum variations $(\vec{p})$. If the mass is constant, the variation of the momentum vector translates into the variation of the velocity vector $(\vec{v})$. Given the symmetry of the problem, these vectors wobble around the guiding centre with a given pitch angle. Therefore, one can simplify the treatment by replacing the momentum vectors with the pitch angle (ϕ_p) or its cosine $(\mu \equiv \cos \phi_p)$.

The equation reads:

$$\frac{\partial f}{\partial t} + v\mu \frac{\partial f}{\partial z} = \frac{\partial}{\partial \mu} \left(D_{\mu\mu} \frac{\partial f}{\partial \mu} \right) + \frac{\partial}{\partial x} \left(D_{xx} \frac{\partial f}{\partial x} + D_{xy} \frac{\partial f}{\partial y} \right) + \frac{\partial}{\partial y} \left(D_{yx} \frac{\partial f}{\partial x} + D_{yy} \frac{\partial f}{\partial y} \right) , \tag{2.47}$$

where the last two terms with partial derivatives in x and y are zero in the absence of electric fields, as is the case. The Fokker-Planck coefficients $(D_{ab}$ and $D_{\mu\mu})$ describe the general relations

$$D_{ab} = \int_0^\infty dt \left\langle \frac{\partial a(t)}{\partial t} \frac{\partial b(t)}{\partial t} \right\rangle \tag{2.48}$$

and

$$D_{\mu\mu} = \int_0^\infty dt \left\langle \frac{\partial \mu(t)}{\partial t} \frac{\partial \mu(0)}{\partial t} \right\rangle , \tag{2.49}$$

for any generalised coordinates a and b. The integral can be readily identified as Kubo's equation [22]. Here, these coordinates can be the usual spatial coordinates (x, y, z) or the pitch angle[2] (μ). Note that in many cases momentum is one of these generalised coordinates,

---

[2]Formally, the pitch angle is ϕ_p, but for simplicity $\mu \equiv \cos \phi_p$ will also be used to refer to the pitch angle,

with their corresponding terms being part of the Fokker-Planck equation (eq. 2.47).

A logical first attempt to tackle this problem would divide it into two parts, one dealing with the transport parallel to the magnetic field ($\vec{B}_0$), and another one perpendicular to it. Parallel transport is the simplest to solve, as it can be reduced to the treatment of pitch-angle scattering of charged particles streaming along the magnetic field. The perpendicular transport is more complex, as it involves the treatment of the spatial diffusion of the particles, in addition to scattering. The main framework for treating both parallel and perpendicular transport is the so-called quasi-linear theory (QLT), described in the next section.

2.2.3 Quasi-linear theory

QLT is a kind of first-order perturbation theory analogous to the Born approximation in (quantum) scattering theory. It is applicable if the perturbations are small, i.e., if

$$\frac{\delta B}{B} \ll 1 \quad \text{and} \quad \frac{c\delta|E|}{B} \ll 1 \,,$$

(the latter only if small-scale electric fields are present), and if the turbulence is fully developed, which means that the perturbed field spans many scales.

QLT is the most widely-used approach for specifying the diffusion coefficient and relevant transport parameters such as the mean free paths parallel and perpendicular to the mean magnetic fields. It has been shown that QLT leads to infinite mean free paths in the case of perpendicular transport when the pitch angle is $90°$. It is also not valid in the case of particle transport in a two-dimensional turbulence. To solve these problems, a non-linear guiding centre theory has been proposed [26], in order to describe the perpendicular diffusion. Recently the authors of ref. [27] employed the description of spatial separation of magnetic field lines in magnetohydrodynamical turbulence, in order to quantify the divergence of the magnetic field on scales smaller than the injection scale of turbulence; they have shown that this divergence may induce superdiffusion of charged particles perpendicularly to the mean magnetic field. The implications of this superdiffusion to cosmic ray (CR) propagation and acceleration, as well as the corresponding non-thermal emission, must still be explored in depth in astrophysical environments.

The full transportm as described within the framework of QLT depends on the calculation of diffusion coefficients (κ_i). More generally, one can define the **diffusion tensor** ($\vec{\overline{\kappa}}$):

$$\vec{\overline{\kappa}} = \begin{pmatrix} \kappa_{xx} & \kappa_{xy} & \kappa_{xz} \\ \kappa_{yx} & \kappa_{yy} & \kappa_{yz} \\ \kappa_{zx} & \kappa_{zy} & \kappa_{zz} \end{pmatrix} = \begin{pmatrix} \kappa_\perp & \kappa_{as} & 0 \\ -\kappa_{as} & \kappa_\perp & 0 \\ 0 & 0 & \kappa_\parallel \end{pmatrix} \,, \tag{2.50}$$

with κ_{as} representing antisymmetric off-diagonal elements. Here, $\kappa_{as} = 0$ for simplicity, but it can be non-zero if, for example, there are some types of drift. Note that the diffusion tensor ($\vec{\overline{\kappa}}$) if diagonal for axisymmetric turbulence ($\kappa_{xy} = \kappa_{yx} = \kappa_{as} = 0$). Moreover, if diffusion

---

interchangeably. The meaning can be implied from the context.

is purely spatial, i.e., in the absence of momentum diffusion[3], as in the case of the purely magnetic fluctuations ($\delta\vec{E} = 0$) considered here.

For instance, it is possible to show that the Fokker-Planck equation (eq. 2.47) for the parallel transport, generalised to three dimensions, leads to:

$$\frac{\partial \mathfrak{f}(\vec{x}, t)}{\partial t} = \sum_{a=\{x,y,z\}} \kappa_{aa} \frac{\partial^2 \mathfrak{f}(\vec{x}, t)}{\partial x_a^2}, \tag{2.51}$$

whose solution, assuming that all particles were concentrated in a single point space at time $t = 0$, is

$$\mathfrak{f}(\vec{x}, t) = \frac{1}{(2\pi)^{3/2}} \frac{1}{\sqrt{8t^3}} \prod_{a=\{x,y,z\}} \frac{1}{\sqrt{\kappa_{aa}}} \exp\left(-\frac{x_a^2}{4t\kappa_{aa}}\right). \tag{2.52}$$

This can be promptly recognised as a Gaussian with

$$\left\langle x_a^2 \right\rangle = 2t\kappa_{aa}, \tag{2.53}$$

which implies remarkable similarities with the random walk results from §2.2.1.

QLT treats particle transport in the six-dimensional phase space. The pitch angle (or better, its cosine, $\mu \equiv \cos\phi_p$) plays a central role in this treatment, through the Fokker-Planck coefficients. In fact, in addition to the spatial Fokker-Planck coefficients, given by

$$D_{ab}(\mu) = \lim_{t\to\infty} \frac{\langle \Delta x_{aa} \rangle}{2t} = \int_0^\infty \mathrm{d}t\, \langle u_a(t)u_b(0) \rangle \tag{2.54}$$

(for the perpendicular components), there are also the pitch-angle Fokker-Planck coefficients:

$$D_{\mu\mu}(\mu) = \lim_{t\to\infty} \frac{\langle \Delta\mu \rangle}{2t} = \int_0^\infty \mathrm{d}t\, \left\langle \frac{\partial\mu(t)}{\partial t} \frac{\partial\mu(0)}{\partial t} \right\rangle. \tag{2.55}$$

For parallel transport, the corresponding diffusion coefficient ($\kappa_\parallel = \kappa_{zz}$) is:

$$\kappa_{zz} = d_{zz}(t) = \frac{1}{2} \frac{\mathrm{d}\left\langle z^2 \right\rangle}{\mathrm{d}t}. \tag{2.56}$$

Similarly, the perpendicular diffusion coefficient ($\kappa_\perp = \kappa_{xx} = \kappa_{yy}$) can be obtained through the Fokker-Planck coefficients as:

$$\kappa_{ab} = \frac{1}{2} \int_{-1}^{+1} \mathrm{d}\mu\, D_{ab}(\mu), \tag{2.57}$$

where $a, b = \{x, y\}$.

---

[3]Momentum diffusion is a phenomenon analogous to spatial diffusion, but in momentum space. In essence, the momenta of particles composing an ensemble changes due to the action of, for instance, external pressure or shear stress.

2.3 Diffusion of cosmic rays in the Galaxy

Now that the basic concepts of cosmic-ray transport have been introduced, it is possible to delve into the specifics of the propagation of CRs in the Galaxy. The main focus will be on the transport of CRs in the Milky Way, but the same principles can be applied to other astrophysical environments. First, a transport equation will be "derived", to describe the evolution of the number density of charged particles in space, time, and momentum. This is done in §2.3.1 Then this formalism will be applied to the classic leaky box problem, in §2.3.2.

2.3.1 The transport equation

To study how charged particles like CRs move in the Galaxy, a good starting point is the assumption that the total number of particles (N) is conserved, which is mathematically expressed through the continuity equation:

$$\frac{\partial n(\vec{x}, t)}{\partial t} + \vec{\nabla} \cdot \vec{J}(\vec{x}, t) = 0 \,, \tag{2.58}$$

where $\vec{J}(\vec{x}, t)$ is the cosmic-ray current at position $\vec{x}$ and instant t, and $n \equiv N/V$ is the particle density in a volume V. By definition, the gradient of the particle density and the current are related through the diffusion coefficient (or better, diffusion tensor, $\vec{\vec{D}}(\vec{x}, t) = \vec{\vec{D}}(\vec{x})$):

$$\vec{J}(\vec{x}, t) = -\vec{\vec{D}}(\vec{x}) \cdot \vec{\nabla} n(\vec{x}, t) \,. \tag{2.59}$$

By plugging this into eq. 2.58, one arrives at:

$$\frac{\partial n(\vec{x}, t)}{\partial t} = \vec{\nabla} \cdot \left[\vec{\vec{D}}(\vec{x}) \cdot \vec{\nabla} n(\vec{x}, t) \right] \,. \tag{2.60}$$

Eq. 2.60 is only true in the stationary case. There are velocity fields associated with the bulk motion of an ensemble of particles. If the fluid is moving with velocity $\vec{u}(\vec{x})$, the time derivative is a convective derivative. Therefore, the following ad-hoc replacement has to be made:

$$\frac{\partial}{\partial t} \quad \rightarrow \quad \frac{\partial}{\partial t} + \vec{u}(\vec{x}) \cdot \vec{\nabla} \equiv \frac{\mathfrak{D}}{\mathfrak{D} t} \,. \tag{2.61}$$

The full justification for the use of the convection operator will not be given here, but it is described in several textbooks on fluid dynamics. For now, it suffices to adopt the $\frac{\mathfrak{D}}{\mathfrak{D} t}$ simply as a representation for the convective derivative.

Particles with different velocities (or conversely, momenta) may behave differently, such that at this stage it is advantageous to make this explicit by doing $n(\vec{x}, t) \rightarrow n(\vec{p}, \vec{x}, t)$. If this is put into eq. 2.60, one obtains:

$$\frac{\mathfrak{D} n(\vec{p}, \vec{x}, t)}{\mathfrak{D} t} - \vec{\nabla} \cdot \left[\vec{\vec{D}}(\vec{x}) \vec{\nabla} n(\vec{p}, \vec{x}, t) \right] = 0 \,. \tag{2.62}$$

Equation 2.62 captures how a fluid of charged particles with density $n(\vec{p}, \vec{x}, t)$ is transported. The diffusion tensor ($\vec{\vec{D}}(\vec{x})$) encodes properties of the intervening magnetic fields. The bulk motion is determined by the fluid velocity $\vec{u}$. If this process is describing, for instance, cosmic-ray transport in the Galaxy, it is natural to ask how did these particles came to compose the fluid. If there is a source of particles, there is a function $Q_a(\vec{p}, \vec{x}, t)$ describing the injection rate of particles of a given species a per unit time per unit volume. Such terms will be added to the right-hand side of the equations. Now eq. 2.62 becomes

$$\frac{\mathfrak{D} n_a(\vec{p}, \vec{x}, t)}{\mathfrak{D} t} - \vec{\nabla} \cdot \left[\vec{\vec{D}}(\vec{x}) \vec{\nabla} n_a(\vec{p}, \vec{x}, t) \right] = Q_a(\vec{p}, \vec{x}, t). \tag{2.63}$$

Note that now the transport equation is described for individual particle species (e.g., different types of nuclei or charged leptons). The function $Q_a(\vec{p}, \vec{x}, t)$ essentially corresponds to the astrophysical sources of particles of type a.

Observing the existence of a source term in eq. 2.63, it is reasonable to ask whether other source or sinking terms should also be considered. Physically, any type of process that implies non-conservation of the particle number (*for a given particle species*), like decays and spallation processes, can be a sinking process. Decays of particles of type a decrease the particle density by

$$\frac{1}{\gamma \tau_a},$$

where γ is the Lorentz factor of the particle, and τ_a the lifetime of particle a. Similarly, collisions with gas composed of particles of type b decreases the density of particles of type a by

$$\sum_b v n_b(\vec{p}, \vec{x}, t) \sigma_{ab}(\vec{p}, \vec{p}_b) = \sum_b \frac{v}{\lambda_{ab}(\vec{p}, \vec{p}_b)} = \sum_b \frac{1}{\tau_{ab}},$$

wherein σ_{ab} is the cross section for the collision of particles a and b, v is its velocity, λ_{ab} is the mean free path for collisions between a and b, and τ_{ab} the collision rate corresponding to this mean free path. For CR transport in the Galaxy, the relevant targets for interactions are essentially just hydrogen and, to a much smaller extent, helium. The two terms due to decay and collisions will be summed and represented by ξ_a,

$$\xi_a(\vec{p}, \vec{x}, t) = \left[\frac{1}{\gamma \tau_a} + \sum_b \frac{1}{\tau_{ab}} \right] n_a(\vec{p}, \vec{x}, t). \tag{2.64}$$

When a particle of a given species a changes into a', the corresponding equations for a' should be corrected accordingly. Likewise, there is a probability of a nuclear decay from a' to result in a. Therefore, there are other two source-like terms that should be added to the right-hand side of eq. 2.63. Let χ_a denote the sum of these terms. They account the differential

cross section for collisions a and b to generate a', such that χ_a can be written as:

$$\chi_a(\vec{p}, \vec{x}, t) = \sum_{a'} \left[\sum_b v\, n_b(\vec{p}, \vec{x}, t) \underbrace{\int \mathrm{d}p' \frac{\mathrm{d}\sigma_{a'b \to a}(\vec{p}, \vec{p}')}{\mathrm{d}p} + \frac{\eta_{a' \to a}}{\gamma' \tau_{a'}}}_{\sigma_{a'b \to a}} \right] n_{a'}(\vec{p}, \vec{x}, t), \quad (2.65)$$

wherein $p_k = |\vec{p}_k|$, γ' denotes the Lorentz factor of particle species a', and $\eta_{a' \to a}$ designates the branching ratio of the decay channel $a' \to a +$ other particles. The information relevant for computing ξ_a and χ_a, namely interactions and decays, are described in detail in §3.

Therefore, eq. 2.63 becomes:

$$\boxed{\frac{\mathfrak{D} n_a(\vec{p}, \vec{x}, t)}{\mathfrak{D}t} - \vec{\nabla} \cdot \left[\vec{\vec{D}}(\vec{x}) \vec{\nabla} n_a(\vec{p}, \vec{x}, t) \right] = Q_a(\vec{p}, \vec{x}, t) - \xi_a(\vec{p}, \vec{x}, t) + \chi_a(\vec{p}, \vec{x}, t).} \quad (2.66)$$

Note the signs of ξ_a and χ_a, which indicate disappearance and appearance of particles of species a, respectively.

Eq. 2.66 is known as the **diffusion-convection equation**. The derivation as outlined above was based on ref. [28]. Similarly treatment was adopted in, e.g., refs. [29–31]. Note that in this derivation the time and momentum dependence of the diffusion tensor were omitted. This is because the inclusion of more complicated terms like momentum diffusion would defeat the purpose of this non-rigorous yet instructive derivation.

2.3.2 The leaky box model

A useful toy model for understanding the propagation of CRs in the Galaxy is the so-called *leaky box* model [32]. In this model, CRs are assumed to leave the Milky Way after a characteristic escape time scale τ_{esc}. The Galaxy is assumed to be a cylinder of height $2h$ and radius r_{d}. These values are known to be $h \simeq 1$ kpc and $r_{\mathrm{d}} \approx 15$ kpc []. Therefore, because the Galaxy is very thin, it is much more likely that particles will escape upwards or downwards, such that the most important length scale is h, to first approximation. This justifies the one-dimensional treatment put forth in this section.

The escape rate of relativistic CRs from the Galaxy is $\tau_{\mathrm{esc}}^{-1} \ll ch$, which ensures that this treatment is physically sensible, though not accurate. The goal is to obtain a solution for eq. 2.66 using this toy model. The simplest version of this models presumes the particle density depends only on the absolute value of the momentum, such that $n_a(\vec{p}, \vec{x}, \vec{t}) = n_a(\vec{p}) = n_a(p)$.

The left-hand side of eq. 2.66 is composed of the convective derivative and the diffusion-related terms and can be simplified as follows:

$$\frac{\mathfrak{D} n_a}{\mathfrak{D}t} - \vec{\nabla} \cdot \left[\vec{\vec{D}} \vec{\nabla} n_a \right] = \underbrace{\frac{\partial n_a}{\partial t}}_{=0 \text{ (steady state)}} + \underbrace{\vec{u} \cdot \vec{\nabla} n_a - \vec{\nabla} \cdot \left[\vec{\vec{D}} \vec{\nabla} n_a \right]}_{\approx \frac{n_a}{\tau_{\mathrm{esc}}}}.$$

An energy-dependent source term Q_a is considered. The other terms on the right-hand–

side of eq. 2.66 are simplified when the assumption that the gas permeating the Galaxy is made of only hydrogen[4] is adopted. They reduce to

$$\xi_a = \frac{1}{\gamma \tau_a} + \frac{1}{\tau_{a,H}} = \frac{1}{\gamma \tau_a} + \frac{v n_H \sigma_a}{\lambda_{a,H}} \,, \tag{2.67}$$

where the notation $\lambda_{a,H}$ is used to emphasise the interaction of particles of type a with the Galactic gas, and

$$\chi_a = \sum_{a'} v n_H \sigma_{a'H \to a} \, n_{a'} + \sum_{a'} \frac{\eta_{a' \to a}}{\gamma' \tau_{a'}} \, n_{a'} \,. \tag{2.68}$$

Assembling all the terms, the diffusion equation for the leaky box model can be written as:

$$\boxed{\frac{n_a(p)}{\tau_{esc}(p)} = Q_a(p) - \xi_a(p) + \chi_a(p) \,.} \tag{2.69}$$

The contribution of other nuclear species decaying into a (the ξ_a term of eq. 2.66) is here neglected. It is convenient to rewrite this equation in terms of the energy (E) instead of the momentum (p), which is trivial.

Nowadays, there are several improvements over the original (yet remarkably useful) leaky box model [33].

2.3.3 The boron-to-carbon (B/C) ratio

An important astrophysical observable related to Galactic cosmic rays is the boron-to-carbon ratio (B/C ratio). It is a key diagnostic tool for understanding how CRs propagate in the Milky Way.

Carbon nuclei are produced abundantly in many astrophysical environments, being accelerated by supernovae (SNs), among other sources. Boron, on the other hand, is not a primary product of these sources. Instead, it is produced through **spallation** processes involving CNO (carbon, nitrogen, and oxygen) nuclei. Spallation is a type of nucleosynthesis mechanisms wherein two nuclei interact, producing something else after interacting.

The most important channels for boron production are through spallation processes involving carbon and oxygen. The boron-to-carbon ratio is an important observable because it provides an estimate of the average length travelled by cosmic rays. The reason for that is simple: carbon is believed to be produced in astrophysical objects, whereas boron is only produced via spallation processes. In other words, B/C is kind of a proxy for the distance and age of the sources of cosmic rays in the Galaxy. The trajectory length of the CRs depends on the magnetic field. This is how diffusion comes into play, and this the reason why the boron-to-carbon ratio is a proxy for the diffusion coefficient.

Consider the nucleus of boron, whose predominant stable isotope is ^{11}B. Suppose no astrophysical sources produce boron. The most important channels for boron production is through spallation processes involving carbon and oxygen. Now apply eq. 2.69 to it in the

---

[4]This is reasonable considering that hydrogen does compose more than 80% of the Galactic matter content.

absence of a source term:

$$\frac{n_B(E)}{\tau_{esc}(E)} + \frac{v n_B(E)}{\lambda_B(E)} = v n_H \left[\sigma_{C \to B} n_C(E) + \sigma_{O \to B} n_O(E) \right] . \tag{2.70}$$

By defining the escape length as

$$\lambda_{esc}(E) \equiv v \tau_{esc}(E) , \tag{2.71}$$

and noting that carbon and oxygen are found in roughly the same amount (i.e., $n_C \approx n_O$), the equation reduces to

$$\frac{n_B(E)}{n_C(E)} \simeq \frac{v n_H}{\frac{1}{\tau_{esc(E)}} + \frac{v}{\lambda_B(E)}} \sigma_{C \to B} + \sigma_{O \to B} . \tag{2.72}$$

The boron-to-carbon ratio (often symbolised by B/C) is an important observable because it provides an estimate of the average length travelled by CRs. The reason for that is simple: carbon is believed to be produced in astrophysical objects, whereas boron is only produced via spallation processes. In other words, B/C is kind of a proxy for the distance and age of the sources of cosmic rays in the Galaxy. The trajectory length of the CRs depends on the magnetic field. This is how diffusion comes into play, and this the reason whereby the boron-to-carbon ratio is a proxy for the diffusion coefficient.

Cosmic-ray deflections in magnetic fields depend on the charge of the particle. In the case of an atomic nucleus of mass A and atomic number Z, the charge is Ze. A convenient definition is the **rigidity**, defined as

$$\boxed{\mathcal{R} = \frac{pc}{Ze} = \frac{A}{Z} \sqrt{E_{kin}^2 + 2 m_p c^2 E_{kin}} ,} \tag{2.73}$$

which also establishes a connection between momentum and kinetic energy per nucleon (E_{kin}).

Recalling §2.1.2, in particular eq. 2.43, there is a general dependence of the average displacement of a particle (actually, the square of it, $\langle r^2 \rangle$) on time for different diffusion regimes:

$$\langle r^2 \rangle \propto t^\chi$$

This directly connects to the diffusion coefficient (eq. 2.44 and 2.46). By fitting the experimental data (see fig. 2.1), it is possible to constrain the diffusion coefficient. In general, it is commonly assumed that the diffusion coefficient has the form

$$D \propto \mathcal{R}^\delta . \tag{2.74}$$

The symbol δ, used here to designate the diffusion index, is adopted only for consistency with most the literature. It is simply $\delta = \alpha_B + 1$, with the magnetic spectral index (α_B).

This rigidity dependence leads to differences at low and high energies since energy does not scale with it linearly. Knowing all cross sections and having measured the boron-to-carbon ratio,

it is possible to infer the index δ and hence α_B. This is the goal of many recent publications in the literature [], which make use of measurements from cosmic-ray satellites such as Payload for Antimatter Matter Exploration and Light-nuclei Astrophysics (PAMELA) and the Alpha Magnetic Spectrometer (AMS). In fact, results by AMS-02 are in excellent agreement with a Kolmogorov-type turbulent spectrum with $\delta = 0.333 \pm 0.014(\text{fit}) \pm 0.005(\text{syst})$ [34]. Note that the low- and high-energy behaviour of δ are different. At much higher energies, $\delta \simeq 0.6$ [].

Having inferred the magnetic spectrum from observations, it is possible to compute the number density of each particle species as in eq. 2.69 for any primary nucleus a. Consider a particular nucleus that is produced in astrophysical objects such that the source term is non-zero $(Q_a(E) \neq 0)$ whose flux is not significantly affected by the decay of other nuclei. It is possible to show that

$$n_a(E) = \frac{Q_a(E)\tau_{\text{esc}}(E)}{1 + \frac{1}{\lambda_a}\lambda_{\text{esc}}(E)} \, . \tag{2.75}$$

Note that once the diffusion coefficient is computed, rigidity and energy can be used interchangeably.

If the source (or sources) emits a power-law spectrum of the form

$$Q_a(E) \propto E^{-\alpha_{\text{src}}} \, , \tag{2.76}$$

having measured a power-law spectrum of the form

$$n_a(E) \propto E^{-\alpha_{\text{obs}}} \, , \tag{2.77}$$

eq. 2.75 leads to

$$\alpha_{\text{src}} = \alpha_{\text{obs}} + 1 - \delta = \alpha_{\text{obs}} - \alpha_B \, . \tag{2.78}$$

Analyses of measurements suggest $\alpha_{\text{src}} \approx 2.1$ []. Note that this generally agrees with the well-known Fermi mechanism, described in 1.1.

A measurements of the B/C ratio by Alpha Magnetic Spectrometer (AMS) are shown in fig. 2.1. The data is consistent with a power-law index of $\delta \approx -0.33$ at the energies indicated by the red line (see eq. 2.74). This offers valuable insights into the diffusion of CRs in the Galaxy. In particular, it is notably consistent with Kolmogorov's turbulence theory [35], which predicts $\delta = -\frac{1}{3}$.
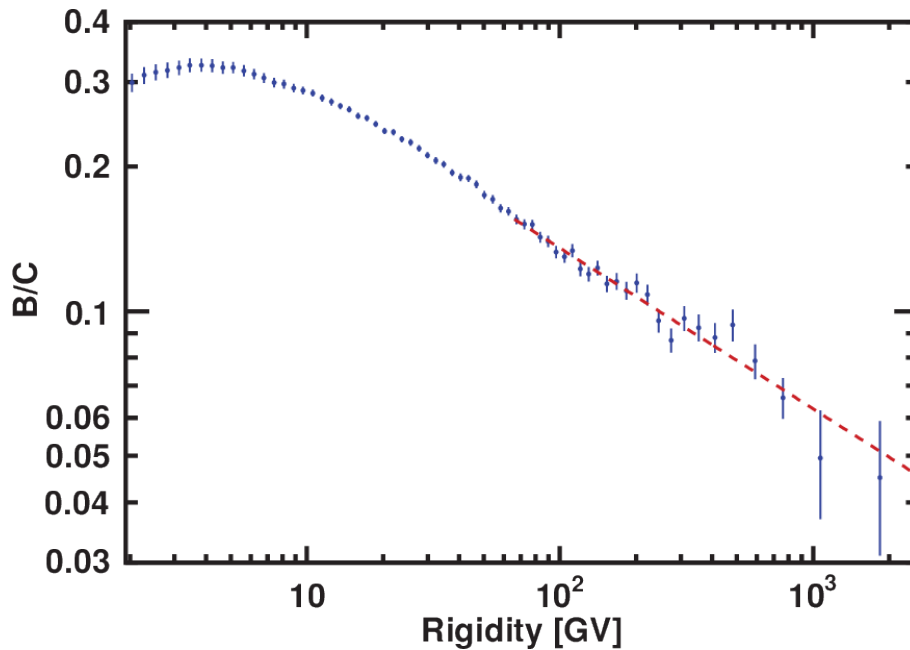
2.3.4   The positron fraction

Figure 2.1: The boroon-to-carbon ratio measured by AMS. Figure taken from [34].

2.4 Exercises

2.1 A charged particle of mass m and charge q moves in a uniform magnetic field $\vec{B} = B_0 \hat{z}$. Assume there are no magnetic fields.
(a) Write down the Lorentz force equation for the particle.
(b) Solve the equations of motion assuming the initial velocity $\vec{v}_0$.
(c) Show that the particle follows a helical trajectory.
(d) Compute the Larmor radius R_L for this particle.

2.2 A population of charged particles moves in a uniform magnetic field $\vec{B} = B_0 \hat{z}$, experiencing small-angle scattering due to interactions with magnetic turbulence. Suppose the particles do not diffuse in the direction perpendicular to the magnetic field, i.e., $D_{xy} = D_{yx} = D_{xx} = D_{yy} = 0$.
(a) Write down the Fokker-Planck equation for the particle distribution function $f(\mu, t)$ in pitch-angle space, where $\mu = \cos \phi_p$, with $\phi_p \equiv \arctan(v_\perp / v_\|)$.
(b) Assume a constant diffusion coefficient $D_{\mu\mu} = D_0$. Find the stead-state solution $f(\mu)$ for this equation.
(c) Is there a physical condition that should be imposed on the solution to item (b) to ensure that $f(\mu)$ is "well-behaved"?
(d) Now, suppose that at $t = 0$ all particles are emitted exactly in the direction of the magnetic field, such that $f(\mu, 0) = \delta(\mu - 1)$, where δ refers to the Dirac delta function. Solve the equation for $f(\mu, t)$. *Hint:* Use the ansatz of a random-walk diffusion solution (see eq. 2.40).
(e) What is the physical meaning of the solution obtained in item (d)?

2.3   Consider a time-independent version of the diffusion-convection equation:

$$\frac{\mathfrak{D}n_a(\vec{p}, \vec{x}, t)}{\mathfrak{D}t} - \vec{\nabla} \cdot \left[\overset{\leftrightarrow}{D}(\vec{x})\vec{\nabla}n_a(\vec{p}, \vec{x}, t)\right] = Q_a(\vec{p}, \vec{x}, t) - \xi_a(\vec{p}, \vec{x}, t) + \chi_a(\vec{p}, \vec{x}, t)\,.$$

(a) Suppose there are no interactions nor decays, and consider that the system is in a steady state. Write the equation explaining the simplifications made.

(b) Write the corresponding differential equation in one dimension, explaining the assumptions made. Use cylindrical galactocentric coordinates.

(c) Solve the equation derived in item (b) above and below the Galactic plane.

(d) Derive a steady-state solution for the equation in item (b).

(e) Sketch the solution for the steady-state solution in item (d) as a function of the distance from the Galactic plane.

2.4   Show that the power-law index of the source spectrum is related to the observed spectrum through the equation:

$$\alpha_{\mathsf{src}} = \alpha_{\mathsf{obs}} + 1 - \delta\,,$$

where α_{src} is the power-law index of the source spectrum, α_{obs} is the observed spectrum, and δ is the index of the rigidity dependence of the diffusion coefficient.

Interactions, decays, and other processes

Some particles do not propagate in a straightforward manner. In certain environments, they can be considerably influenced by external factors such as magnetic fields or interactions with other particles. These settings encompass intergalactic space, the vicinity of astrophysical objects, our own galaxy, and even Earth's atmosphere. The fundamental principles that describe these processes remain consistent, regardless of the specific environment in which they take place. This section provides a comprehensive overview of some of these principles, which are relevant for the propagation of high-energy astroparticles.

3.1 Basic concepts

3.1.1 Kinematics of 2-body interactions

The interaction between two particles can be modelled within the framework of (special-)relativistic kinematics.

Consider an interaction between any two particles '1' and '2' with masses m_1 and m_2, respectively. Their four-vectors are $P_1 = (E_1/c, \vec{p}_1)$ and $P_2 = (E_2/c, \vec{p}_2)$, wherein E denotes the energy and $\vec{p}$ the momentum in the *laboratory frame*.

The squared centre-of-mass energy $(s \equiv E_{\text{CM}}^2)$ is a relativistic invariant. For the centre-of-mass, this invariant reads

$$s = E_{\text{CM}}^2 = (E_1 + E_2)^2 - (\vec{p}_1 + \vec{p}_2)^2 \, c^2 \,, \tag{3.1}$$

which reduces to

$$s = m_1^2 c^4 + m_2^2 c^4 + 2E_1 E_2 \left(1 - \beta_1 \beta_2 \cos\theta\right) \,. \tag{3.2}$$

Here $\beta \equiv v/c$ refers to the speed of the particle, and θ is the angle (in the lab frame) between the two particles.

A remarkable feature of equation 3.2 is that it does not depend on the outcomes of the

process of interest. It can be used generically for any two particles.

3.1.2 Cross sections

A generic process $A + B \to \mathrm{f}$ characterises **elastic scattering** if the final state (f) is composed by the same initial particles (A and B) and no other, which simply means they exchanged momentum among themselves. In **inelastic scattering** the particles A and B are not necessarily part of the final state (f).

The **total cross section** (σ_tot) is defined as the sum of the cross sections for elastic (σ_ela) and inelastic scattering (σ_ine):

$$\sigma_\mathrm{tot} = \sigma_\mathrm{ela} + \sigma_\mathrm{ine} \,. \tag{3.3}$$

Inelastic scattering lead to the creation of secondary particles (C): $A + B \to C + \ldots$. The **inclusive cross section** describes exactly this reaction, ignoring all other channels such as $A + B \to D + \ldots$, and so on. In contrast, **exclusive cross sections** include all possible by-products of the interaction: $A + B \to C + D + \ldots$.

Inheriting from the mathematical formalism commonly employed in accelerator physics, it is convenient to consider the laboratory frame. In this frame the notation $\mathrm{p} + \mathrm{t} \to \mathrm{f}$ is simpler, wherein p refers to the incident particles (projectiles) and t denotes the target; f still denotes an arbitrary final state, as before. Now the cross section for this process can be defined as [28]

$$\sigma_{\mathrm{p}+\mathrm{t}\to\mathrm{f}} = \frac{1}{\Phi_i} \frac{\mathrm{d}N_f}{\mathrm{d}t} \,, \tag{3.4}$$

where Φ_p is defined as in eq. **??**. The final state can take various values for the momentum ($\vec{p}_f$). This is captured by the **differential cross section**:

$$\frac{\mathrm{d}^3 \sigma_{\mathrm{p}+\mathrm{t}\to\mathrm{f}}}{\mathrm{d}^3 \vec{p}_\mathrm{f}} = \frac{1}{\Phi_\mathrm{p}} \frac{\mathrm{d}^4 N_f}{\mathrm{d}^3 \vec{p}_\mathrm{f} \, \mathrm{d}t} \,. \tag{3.5}$$

Here the cross section is *inclusive*. The exclusive cross section for a process $\mathrm{p} + \mathrm{t} \to f_1 + f_2 + \ldots + f_j$, where j denotes the number of secondaries, can be written by a generalisation of the equation above:

$$\frac{\mathrm{d}^3 \sigma_{\mathrm{p}+\mathrm{t}\to f_1+\ldots+f_j}}{\mathrm{d}^3 \vec{p}_\mathrm{f}} = \frac{1}{\Phi_\mathrm{p}} \frac{\mathrm{d}^{3j+1} N_\mathrm{f}}{\mathrm{d}^3 \vec{p}_{\mathrm{f}_1} \ldots \mathrm{d}^3 \vec{p}_{\mathrm{f}_j} \, \mathrm{d}t} \,. \tag{3.6}$$

3.2 Radiation from moving charges

3.2.1 General formulation

The Larmor formula [36] for the power ($\mathrm{d}E/\mathrm{d}t$) radiated by a charged particle of charge q and mass m moving with acceleration $\vec{a}$ is given by:

$$\frac{\mathrm{d}E}{\mathrm{d}t} = -\frac{q^2 a^2}{6\pi\varepsilon_0 c^3} \,, \tag{3.7}$$

where ϵ_0 is the vacuum permittivity, and c is the speed of light. The acceleration $\vec{a}$ is related to the position by $\vec{a} = \ddot{\vec{r}}$. The power radiated by a moving charge is proportional to the square of the acceleration, and it is emitted in the form of electromagnetic radiation.

This expression can be easily generalised to the relativistic case:

$$\frac{\mathrm{d}E}{\mathrm{d}t} = -\frac{q^2 \gamma^4}{6\pi\varepsilon_0 c^3} \left(\gamma^2 |a_\parallel|^2 + |a_\perp|^2 \right) , \tag{3.8}$$

where $a_\parallel$ and $a_\perp$ refer to the components of the acceleration parallel and perpendicular to the particle's velocity, respectively.

Compare eq. 3.8 with eq. 3.7. It is straightforward to see that for low velocities $\gamma \sim 1$ and the two formulas are equal to each other. However, there is a remarkable change in the relativistic case, where the power radiated by the particle is proportional to several powers of the Lorentz factor γ. This is a direct consequence of the relativistic effects on the particle's mass and velocity.

The angular distribution of the emitted radiation depends on the solid angle (Ω) between the acceleration and the velocity of the particle and is given by:

$$\frac{\mathrm{d}^2 E}{\mathrm{d}t\,\mathrm{d}\Omega} = \frac{q^2}{16\pi^2\varepsilon_0 c} \frac{\left| \hat{\varrho} \times \left[(\hat{\varrho} - \vec{\beta}) \times \dot{\vec{\beta}} \right] \right|^2}{(1 - \hat{\varrho} \cdot \vec{\beta})^5} , \tag{3.9}$$

where $\hat{\varrho}$ represents the unit vector pointing from the charge to the observer, and $\dot{\vec{\beta}}$ is the temporal derivative of the (normalised) velocity $\vec{\beta}$. The term within square brackets encodes the angular distribution of the emitted radiation, as well as the polarisation.

Note that eq. 3.9 contains a term that depends on the line of sight ($\hat{\varrho}$) with respect to the direction of motion ($\vec{\beta}$). For relativistic particles, the angle denominator ($(1 - \hat{\varrho} \cdot \vec{\beta})$) approaches zero, quickly, implying a strong enhancement of the radiation emitted in the forward direction — the **relativistic beaming**.

The radiation emitted by a moving charge is distributed over a wide range of frequencies. Therefore, it is convenient to express the radiated power in terms of the acceleration's Fourier transform, as done by Longair [7]. Let $\tilde{a}(\omega)$ denote the Fourier transform of the acceleration, for an angular frequency ω. To simplify the notation, I will drop the tilde and refer to the acceleration as a function of time explicitly as $a(t)$, and to its Fourier transform as $a(\omega)$. This relation can be written as:

$$a(t) = \int\limits_{-\infty}^{\infty} \mathrm{d}\omega \, a(\omega) \exp\left(-\mathrm{i}\omega t\right) . \tag{3.10}$$

Total total energy emitted by the particle at a given frequency (ω), is given by [7]:

$$\mathcal{I}(\omega) = \frac{q^2}{3\pi\epsilon_0 c^3} |\vec{a}(\omega)|^2 , \tag{3.11}$$

where $\mathcal{I}(\omega)$ is the intensity of the radiation emitted at a given (angular) frequency throughout the time interval within which the particle undergoes accelerated. It is related to the total power through the expression:

$$\frac{\mathrm{d}E}{\mathrm{d}t} = -\int_0^{E/\hbar} \mathrm{d}\omega \, \mathcal{I}(\omega) \,. \tag{3.12}$$

3.2.2 Bremsstrahlung

Bremsstrahlung, also known as braking radiation, is the radiation emitted by a charged particle under the effect of Coulombian forces from another charged particle. The archetypical case is the deceleration of electrons by atomic nuclei.

Here the results for the more general relativistic case will be presented. Following eq. 3.8, the power radiated by a particle of charge q and mass m moving with acceleration $\vec{a}$ requires the computation of the components of the acceleration parallel and perpendicular to the particle's velocity. Let q' be the charge of the target particle (e.g., the nucleus) and b denote the impact parameter in the classical sense. It is possible to show that the distance between the particle and the target is essentially a right triangle with sides b and $\gamma v t$, where v is the velocity of the particle and t is the time elapsed since the beginning of the interaction. Therefore, the parallel and perpendicular components of the acceleration are given by [7]:

$$a_\parallel = \frac{qq'\gamma}{4\pi\varepsilon_0 m} \frac{vt}{R^3} \,, \tag{3.13}$$

$$a_\perp = \frac{qq'\gamma}{4\pi\varepsilon_0 m} \frac{b}{R^3} \,, \tag{3.14}$$

where $R \equiv \sqrt{b^2 + (\gamma v t)^2}$.

The power radiated is obtained by plugging these expressions into eq. 3.8:

$$\frac{\mathrm{d}E}{\mathrm{d}t} = -\frac{q^4 q'^2}{96\pi^3 \varepsilon_0^3} \frac{\gamma^4}{m^2 c^3} \frac{1}{R^3} \left(b^2 + v^2 t^2 \right) \,. \tag{3.15}$$

The total energy radiated by the particle is given by eq. 3.11 [7]:

$$\mathcal{I}(\omega) = \frac{q^4 q'^2}{24\pi^4 \varepsilon_0^3} \frac{\omega^2}{m^2 c^3 v^4} \frac{1}{\gamma^4} \left[K_0^2(\upsilon) + \gamma^2 K_1^2(\upsilon) \right] \,, \tag{3.16}$$

where $\upsilon = \frac{\omega b}{\gamma v}$, and K_0 and K_1 represent the modified Bessel functions of the second kind of order zero and one, respectively. The second term within square brackets refers to the contribution of the parallel component of the acceleration, whereas the first refers to the perpendicular component.

42

3.2.3 Synchrotron radiation

When exposed to a magnetic field, charged particles can release synchrotron radiation. The radiated power is given by eq. 3.8, where the acceleration is now the centripetal acceleration of the particle moving in a circular path due to the magnetic Lorentz force. In this case, the acceleration is perpendicular to the direction of motion, such that $a_\parallel = 0$ and

$$a_\perp = \frac{q}{m\gamma}|\vec{v} \times \vec{B}| \tag{3.17}$$

For a particle of mass m and charge q, moving with velocity $\vec{v}$, the energy loss per unit time is given by:

$$\frac{\mathrm{d}E}{\mathrm{d}t} = -\frac{q^4}{6\pi\epsilon_0}\frac{1}{c^3 m^2}(\gamma v B \sin\theta)^2 \,, \tag{3.18}$$

where ϵ_0 denotes the vacuum permittivity, and $\vec{B}$ represents the magnetic field. Here, θ is the angle formed by the magnetic field with the direction of motion. Note that when the particle's motion aligns with the magnetic field, i.e., $\vec{p} \parallel \vec{B}$, no radiation is emitted.

For an ultrarelativistic electron, eq. 3.18 can be cast into a form that contains the magnetic energy density ($u_B = B^2/2\mu_0$):

$$\frac{\mathrm{d}E}{\mathrm{d}t} = -2\sigma_\mathrm{T}u_B c\gamma^2 \sin^2\theta \,, \tag{3.19}$$

where σ_T is the Thomson cross section, defined in §3.3.1.

The intensity of the radiation emitted by the particle is given by eq. 3.11, which leads to the following results:

$$\mathcal{I}_\parallel(\omega) = \frac{\sqrt{3}q^2}{8\pi\varepsilon_0 c}\frac{\omega}{\omega_\mathrm{c}}\gamma\sin\theta\left[\frac{1}{\omega_\mathrm{c}}\int_{\omega/\omega_\mathrm{c}}^{\infty} K_{5/3}\left(\frac{\omega'}{\omega_\mathrm{c}}\right)\mathrm{d}\omega' - K_{2/3}\left(\frac{\omega}{\omega_\mathrm{c}}\right)\right] \,, \tag{3.20}$$

$$\mathcal{I}_\perp(\omega) = \frac{\sqrt{3}q^2}{8\pi\varepsilon_0 c}\frac{\omega}{\omega_\mathrm{c}}\gamma\sin\theta\left[\frac{1}{\omega_\mathrm{c}}\int_{\omega/\omega_\mathrm{c}}^{\infty} K_{5/3}\left(\frac{\omega'}{\omega_\mathrm{c}}\right)\mathrm{d}\omega' + K_{2/3}\left(\frac{\omega}{\omega_\mathrm{c}}\right)\right] \,, \tag{3.21}$$

where $K_{5/3}$ and $K_{2/3}$ are modified Bessel functions of the second kind of order 5/3 and 2/3, respectively. Here ω_c is the **critical frequency** (actually, angular frequency) of the emitted synchrotron radiation, given by:

$$\omega_c = \frac{3c}{2v}\frac{|q|B}{m}\gamma^3 \sin\theta \,. \tag{3.22}$$

For the full derivation, see the detailed discussion in chapter 8 of Longair [7][1].

Synchrotron radiation plays a central role in the study of astrophysical sources. On one

---

[1]In the book, Longair [7] introduces many intermediate variables whose explanations and/or derivations only become clear several pages later. I opted for already introducing the meaningful physical quantities from the start, and writing everything in terms of them, namely the critical frequency.

hand, it can be the dominant energy-loss mechanism of charged particles, decreasing their energy and counter-acting possible energy gains due to acceleration. On the other hand, it is thanks to synchrotron emission that it is possible to infer the properties of magnetic fields in astrophysical sources [37], and also identify particle acceleration in astrophysical shocks (see, for instance, fig. 1.3).

3.3 Electromagnetic interactions

3.3.1 Thomson scattering

Thomson[2] scattering is the elastic scattering of photons by a (free) charged particle ($X^{\pm}$):

$$X^{\pm} + \gamma \rightarrow X^{\pm} + \gamma\,. \tag{3.23}$$

It happens when the energy of the photons is much less than than the particle's energy in its own rest frame, such that a non-relativistic treatment is appropriate. In fact, Thomson scattering can be seen as the classical limit of Compton scattering wherein the photon energy is conserved. The scattering cross section for this process is given by

$$\sigma = \frac{8\pi}{3} \left(\frac{q^2}{4\pi\varepsilon_0 m c^2} \right)^2\,. \tag{3.24}$$

For electrons, this cross section is known as the Thomson cross section (σ_{T}),

$$\boxed{\sigma_{\mathsf{T}} = \frac{8\pi}{3} \left(\frac{e^2}{4\pi\varepsilon_0 m_e c^2} \right)^2 \approx 6.65 \times 10^{-29} \text{ m}^2\,.} \tag{3.25}$$

Intuitively, Thomson scattering can be viewed as an interaction between a light a charged dipole, representing the particle. Mathematically, the derivation follows along these lines, considering the electromagnetic field of the charge in the dipolar approximation. The light excites the dipole, which then re-radiates. One of the most important characteristics of the emitted radiation is that it is *polarised* in the direction of motion, with most power being radiated perpendicular to the direction of acceleration.

Unlike Compton scattering, Thomson scattering is not a quantum process. It is a classical effect, and it is the simplest interaction between light and matter. The particles involved do not change their energy.

Thomson scattering is responsible for generating polarised radiation in a variety of astrophysical settings. For example, the cosmic microwave background (CMB) has $\sim 10\%$ linear polarisation which affects the so-called E-modes[3]. While this offers direct hints of the processes

---

[2]It is common to misattribute this effect to certain 'Thompson'. This is historically incorrect. This scattering is named after J. J. Thomson, who first calculated this effect in detail in his 1906 book "Conduction of electricity through gases".

[3]

taking place in the early universe, which led to this phenomenon, it also acts as backgrounds in the study of other phenomena, such as the stochastic gravitational wave (GW) background [].

3.3.2 Breit-Wheeler pair production

Breit-Wheeler pair production is one of the simplest processes in quantum electrodynamics (QED). It is essentially the direct production of an electron-positron pair due to the interaction of two photons [38]:

$$\gamma + \gamma_{\text{bg}} \rightarrow e^+ + e^- \, , \tag{3.26}$$

where γ_{bg} refers to a background photon (e.g., CMB, extragalactic background light (EBL)). The cross section, shown in fig. 3.25 for this process is:

$$\sigma(\beta) = \frac{3\sigma_{\text{T}}}{16} \left(1 - \beta^2\right) \left[\left(3 - \beta^4\right) \ln\left(\frac{1+\beta}{1-\beta}\right) - 2\beta\left(2 - \beta^2\right) \right] \, , \tag{3.27}$$

where σ_{T} represents the Thomson cross section (see eq. **??**), and

$$\beta = \sqrt{1 - \frac{4m_e^2 c^4}{s}} \, . \tag{3.28}$$

Here s is the squared centre of mass energy, which for a high-energy photon with energy E scattering off a low-energy background photon of energy ε reads

$$s = 2E\varepsilon\left(1 - \cos\theta\right) \, , \tag{3.29}$$

wherein θ denotes the collision angle. It follows immediately that the kinematic thresholds for this interaction are $s_{\text{min}} = m_e^2 c^4$ and $s_{\text{max}} = m_e^2 c^4 + 2E\varepsilon_{\text{max}}(1+\beta)$.
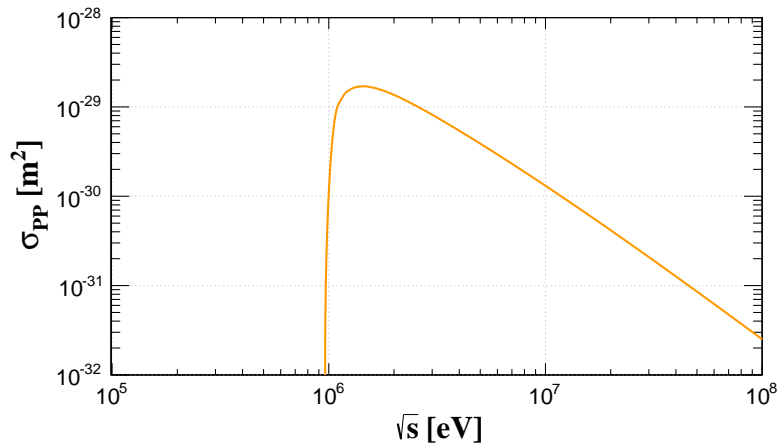

Figure 3.1: Cross section for pair production as a function of the centre-of-mass energy of the produced particles. Figure taken from ref. [39].

It is natural to think that electrons and positrons will have approximately the same energy. In the high-energy regime ($s \gg m_e^2 c^4$), also known as the Klein-Nishina limit, this is not

necessarily true. In this case, the energy of the leptons produced will depend on the differential cross section for the process:

$$\frac{\mathrm{d}\sigma}{\mathrm{d}y} \propto \frac{1}{y}\left[\frac{y^2}{1-y}+1-y+\frac{(1-\beta^2)^2}{4y(1-y)^2}\right]\frac{1}{1+2\beta^2-2\beta^4}\,, \tag{3.30}$$

where y is the fraction of the energy of the energetic photon being taken by one of the particles produced. The other particle, evidently, takes a fraction of the primary's energy of $1-y$.

3.3.3 (Inverse) Compton scattering

This basic QED process is described by the reaction:

$$e^{\pm} + \gamma_{\mathrm{bg}} \to e^{\pm} + \gamma\,. \tag{3.31}$$

Inverse Compton scattering (ICS) is, therefore, a simple momentum exchange, as is the usual Compton effect [40], but in this case involving a high-energy electron and low-energy photons instead of the opposite. *Compton effect*, both the direct and the inverse, constitute one of the most important milestones of 20th-century physics [41] with far-reaching consequences in several sub-fields of physics, especially astrophysics.

The squared centre-of-mass energy (s) is

$$s = m_e^2 c^4 + 2E\varepsilon\left(1-\beta\cos\theta\right)\,, \tag{3.32}$$

with β given by

$$\beta = \frac{s-m_e^2 c^4}{s+m_e^2 c^4}\,. \tag{3.33}$$

Its kinematic threshold is simply the requirement that the electron continues to exist after the collision: $s_{\mathrm{min}} = m_e^2 c^4$.

The cross section for ICS can be written as [42]

$$\sigma(s) = \frac{3\sigma_T}{8\beta}\frac{m_e^2 c^4}{s}\left[\frac{2}{\beta(1+\beta)}(2+2\beta-\beta^2-2\beta^3)-\frac{1}{\beta^2}(2-3\beta^2-\beta^3)\ln\left(\frac{1+\beta}{1-\beta}\right)\right]\,. \tag{3.34}$$

In the low-energy limit ($s \sim m_e^2 c^4$), eq. 3.34 reduces to the usual Thomson scattering result, given by eq. 3.25.

After the scattering the electron (or positron), which had an initial energy E, will have energy E', as dictated by the differential cross section [43]:

$$\frac{\mathrm{d}\sigma}{\mathrm{d}E'} = \frac{3\sigma_T}{8E}\frac{m_e^2 c^4}{s}\frac{1+\beta}{\beta}\left[y+\frac{1}{y}+\frac{2(1-\beta)}{\beta}\left(1-\frac{1}{y}\right)+\frac{(1-\beta)^2}{\beta^2}\left(1-\frac{1}{y}\right)^2\right]\,, \tag{3.35}$$
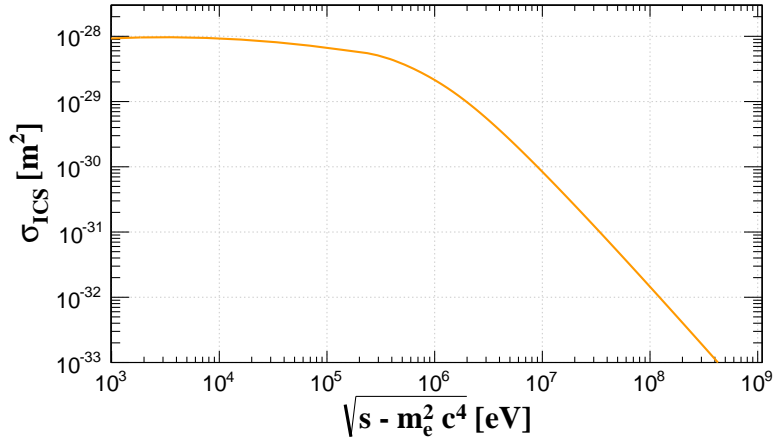
with $y \equiv E'/E$.

Figure 3.2: Cross section for inverse Compton scattering as a function of the kinetic centre-of-mass energy of the produced particles. Figure taken from ref. [39].

3.3.3.1 Synchrotron self-Compton

In the presence of magnetic fields, electrons can emit synchrotron radiation (see §3.2.3). If this happens at a sufficiently high rate, the density of synchrotron-emitted photons in the medium can increase, creating a new target for interactions. If electrons scatter off this radiation field, created by themselves, the process is known as synchrotron self-Compton (SSC). This is a crucial process in the context of high-energy astrophysics, especially in the study of active galactic nuclei (AGNs) and gamma-ray bursts (GRBs).

3.4 Photonuclear interactions

Photonuclear interactions involve the interaction of a nucleus X, with atomic mass A, composed of Z protons ($^A_Z X$). They are generally written as $^A_Z X + \gamma_{bg} \to \dots$. The exact interaction taking place depends on the cross section for the processes, which is a consequence of the spectral energy distribution of background photons (γ_{bg}) and on the energy of the nucleus. The ellipsis ('...') indicate the results of the interaction, which depends on the spectral distribution of background photons as well as on the energy of the nucleus. Some of the processes relevant for high-energy modelling are listed below

3.4.1 Bether-Heitler pair production

When a nucleus interacts with a background photon (γ_{bg}) electron-positron pairs can be created [44]. This is described by the reaction:

$$^A_Z X + \gamma_{bg} \to {}^A_Z X + e^+ + e^- .$$ (3.36)

It is essentially the equivalent to bremsstrahlung radiation with a photon instead of an electron/positron on the left side of the reaction, which is expected for symmetry reasons.

The threshold squared centre-of-mass energy for this process is given by

$$s_{\text{min}} = (m_X + 2m_e)^2 \,, \tag{3.37}$$

which implies that the minimum energy $(\varepsilon_{\text{min}})$ of the background photon, measured in the lab frame, is

$$\varepsilon_{\text{min}} = \frac{m_e c^2}{2E} \left(2m_e^2 + m_e m_X \right) c^2 \,, \tag{3.38}$$

wherein the E denotes the energy of the incident nucleus.

For UHECRs traversing cosmic expanses, the mean free path for Bethe-Heitler pair production is fairly small, but so is the inelasticity of the process ($\lesssim 10^{-3}$).

[add figure for each type of background]

Remarkably, it has been postulated that this process underlies the origin of the *ankle* feature in the cosmic-ray spectrum if protons comprise the bulk of the UHECR flux [45], which is not the case [46].

3.4.2 Meson photo-production

The generation of mesons resulting from the interaction between a cosmic-ray nucleus $\left(^A_Z X\right)$ and a background photon (γ_{bg}) holds immense significance within the multi-messenger framework, as it yields both neutrinos and photons. For instance, when considering protons, in their rest frame, the interaction with photons with energies $\varepsilon' \gtrsim 1$ GeV is characterised by the dominance of a short-lived resonance, which rapidly transforms into mesons and other secondary particles. As energy levels escalate, the potential for multiple particle generation during a single interaction also increases. Furthermore, direct meson production is feasible at these elevated energies.

$$p + \gamma_{\text{bg}} \to \Delta^+ \to \begin{cases} p + \pi^0 \,, \\ n + \pi^+ \,. \end{cases} \tag{3.39}$$

Naturally, there are also channels that produce, for example, Δ^- or Δ^0 resonances, and even higher-order excitations.

The cross section for the interaction between a nucleon and a background photon in the rest frame of the nucleon is shown in Fig. 3.3.

The total proton-photon cross section is in reality a combination of several processes, some of which involve the direct production of single or multiple pions, or other resonances. The bumpy structure visible in fig. 3.3 is actually the result of these components, which are identified in fig. 3.4.

Considering a proton, the threshold for this process is

$$s_{\text{min}} = (m_p + m_{\pi^0})^2 c^4 \,, \tag{3.40}$$

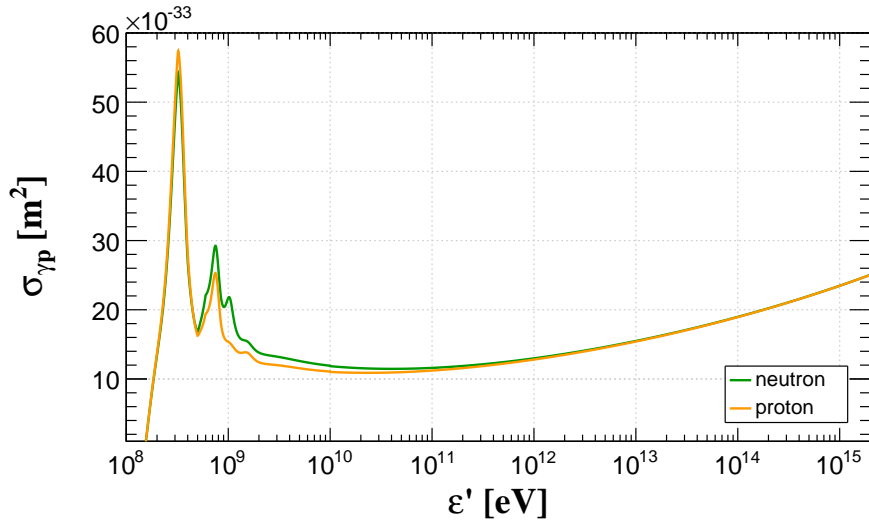Figure 3.3: The graph shows the total cross section for $p + \gamma_{\text{bg}} \to$ meson (orange line) and $n + \gamma_{\text{bg}} \to$ meson (green line), as a function of the background photon energy in the nucleon rest frame (ε'). Figure taken from ref. [39].
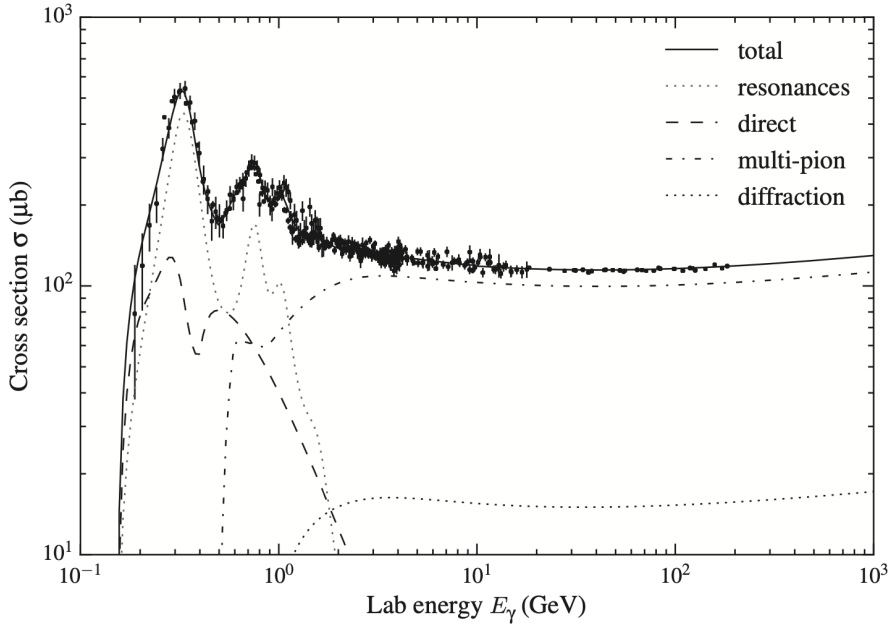

Figure 3.4: Total cross section for $p + \gamma_{\text{bg}} \to$ meson, as a function of the background photon energy in the nucleon rest frame. Figure taken from ref. [28].

which implies that the threshold energy for a proton (E), measured in the lab frame, is

$$E_{\min} = \frac{m_{\pi^0} c^2}{4\varepsilon} \left(2m_p + m_{\pi^0} \right) c^2 . \tag{3.41}$$

For a CMB photon, the peak energy is $\varepsilon \approx 6 \times 10^{-4}$ eV, which implies $E_{\min} \sim 10^{20}$ eV.

Photo-production of mesons is a crucial process in the context of UHECR propagation.

It is responsible for the well-known Greisen-Zatsepin-Kuzmin (GZK) cut-off in the cosmic-ray spectrum, which implies a spectra feature as a consequence of the energy loss of UHECR protons interacting with the CMB [47, 48]. Coincidentally, the spectral suppression measured by UHECR observatories at energies above 5×10^{19} eV roughly coincide with the thresholds calculated above, if the full distribution of the CMB is considered. This is actually the main channel for production of **cosmogenic particles**.

3.4.3 Photodisintegration

Interactions involving cosmic rays and background photons can fragment nuclei into smaller constituents:

$$^{A}_{Z}X + \gamma_{\mathrm{bg}} \rightarrow ^{A'}_{Z'}X + \ldots . \tag{3.42}$$

This phenomenon is usually interpreted as two sequential subprocesses, the first being photo-absorption by the nucleus, which creates an excited state, and its subsequential decay that often emits nucleons [49].

The outcomes of photodisintegration are exemplified by processes such as:

- proton emission: $^{A}_{Z}X + \gamma_{\mathrm{bg}} \rightarrow ^{A-1}_{Z-1}X + p$;
- neutron emission: $^{A}_{Z}X + \gamma_{\mathrm{bg}} \rightarrow ^{A-1}_{Z}X + n$;
- α-particle emission: $^{A}_{Z}X + \gamma_{\mathrm{bg}} \rightarrow ^{A-4}_{Z-2}X + ^{4}_{2}He$.

At ultra-high energies, the photodisintegration cross section is significantly influenced by two components. The first is the giant dipole resonance (GDR), which dominates at photon energies $\varepsilon' \lesssim 50\,\mathrm{MeV}$ in the nucleus rest frame. The other is the quasi-deuteron (QD) emission, prevalent in the energy range $50 \lesssim \varepsilon'/\mathrm{MeV} \lesssim 150$.

Photodisintegration can be viewed as a sort of collective effect, due to the interaction of a photon with a nucleus as a whole. In contrast, photo-production of mesons, described in §3.4.2 is a nucleon-level process. Fig. 3.5 illustrates this difference for an iron nucleus. There is a clear transition between the two regimes. As energy increases, one observes the onset of meson photo-production, whereas for "lower" energies (in the nucleus rest frame), the photon-nucleus interaction is strongly dominated by the GDR.

When modelling photodisintegration processes, it is important to bear in mind that photonuclear cross sections are not fully known. As a consequence, they can have a considerable impact in the propagation of UHECRs [51–53]. Consequently, this knowledge gap holds the potential to substantially impact the consequent production of photons and neutrinos [54].

The threshold energy for photodisintegration depends on the outcomes of the process, such that a universal formula cannot be provided.

3.4.4 Photonuclear elastic scattering

Nuclei can undergo interactions with background photons and simply transfer energy to them. This process is known as elastic scattering: $^{A}_{Z}X + \gamma_{\mathrm{bg}} \rightarrow ^{A}_{Z}X + \gamma$. At ultra-high energies, this is subdominant compared to photodisintegration.
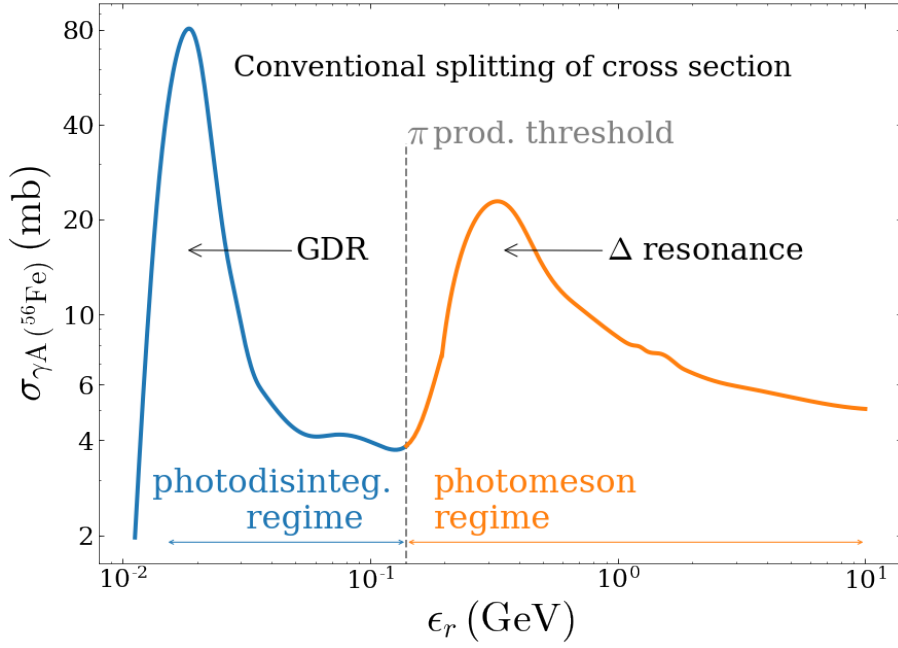
Figure 3.5: Total cross section for $^{56}_{26}$Fe $+ \gamma_{bg} \to \dots$. The left-hand side shows the photo-disintegration regime, whereas the right-hand side indicates the regime in which mesons are produced (called 'photo-meson regime' in the plot). The horizontal axis denotes the photon energy in the nucleus rest frame (ϵ_r). Figure taken from ref. [50].

Elastic scattering is negligible as an energy-loss mechanism of nuclei, but it can be important in computing photon fluxes produced by energetic cosmic-ray nuclei.

3.5 Hadronuclear interactions

Hadronuclear interactions are generally elaborate and cannot be exactly described. This is because the underlying theory of strong interactions, quantum chromodynamics (QCD), poses major challenges in terms of computational treatment.

The simplest case is the interaction between two nucleons. In particular, proton-proton interactions are important in astrophysical constants. There are several possible channels. The overwhelming majority result in the production of pions. Some of these channels are shown below.

$$
p + p \to \begin{cases} p + p + \pi^0 \, , \\ p + p + \pi^0 + \pi^0 \, , \\ p + n + \pi^+ + \pi^0 \, , \\ p + n + \pi^+ + \pi^- + \pi^0 \, . \end{cases} \tag{3.43}
$$

The cross section for proton-proton interactions are not exactly known. Instead, it is obtained through a combination of measurements [55–61] and extrapolation to higher energies using hadronic interaction models [62–65]. Fig. 3.6 shows the measurements, together with some parametrisations.
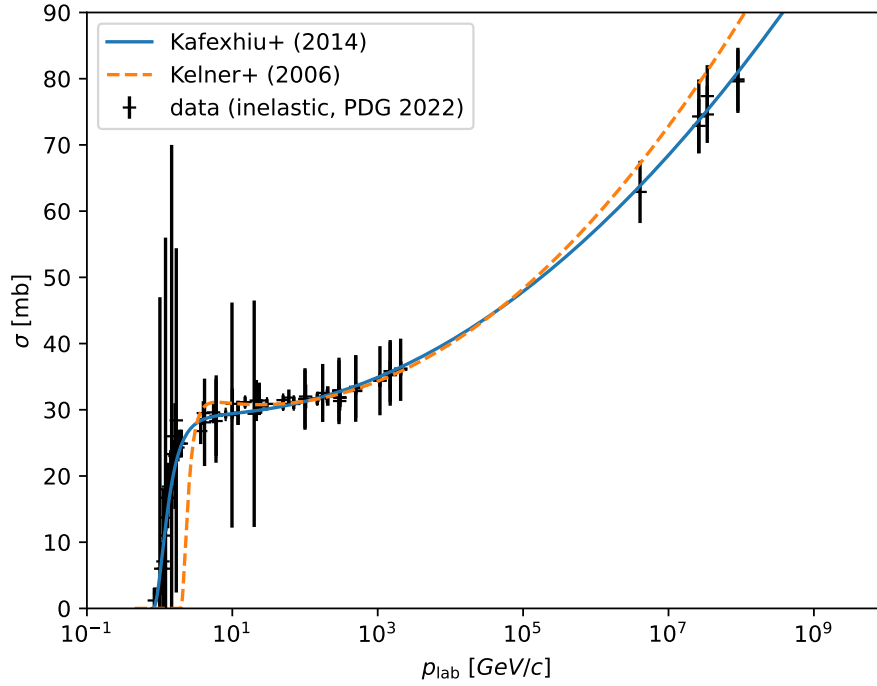
51

Figure 3.6: Inelastic proton-proton cross sections as a function of the momentum of the incident proton. The markers indicate the measurements, whereas the lines refer to some specific parametrisations of the cross section [66, 67]. Figure taken from ref. [**doerner2025a**].

For nucleus-nucleus interactions, Glauber theory [68] can be employed. In this case, the collision can be modelled as a succession of interactions between a nucleon from the projectile with a nucleon from the target nuclei. Even though this is an approximation, it sets an upper limit to the total inelastic cross section, which should be smaller than the sum of all individual nucleon-nucleon cross sections. This approximation is not adequate for lighter nuclei [69].

The nucleus-nucleus cross section can be approximated as [70]

$$\sigma_{\mathrm{ine}}^{A_{\mathrm{p}},A_{\mathrm{t}}}(\chi) = \pi r_0^2 \left[A_{\mathrm{p}}^{1/3} + A_{\mathrm{t}}^{1/3} - b_0 \left(A_{\mathrm{p}}^{-1/3} + A_{\mathrm{t}}^{-1/3} \right) \right] \max \left\{ 1, \log \left(\frac{\sigma_{\mathrm{ine}}^{pp}(\chi)}{\sigma_{\mathrm{ine}}^{pp}(\chi_0)} \right) \right\} , \quad (3.44)$$

wherein A_{p} and A_{t} refer to the atomic mass of the incident and target nuclei, respectively, and the coefficient b_0, empirically obtained, reads [67]

$$b_0 = \begin{cases} 2.247 - 0.915 \left(1 + A_{\mathrm{t}}^{-1/3} \right) & \text{if } \mathrm{p} = {}^1\mathrm{H} , \\ 1.581 - 0.876 \left(A_{\mathrm{p}}^{-1/3} + A_{\mathrm{t}}^{-1/3} \right) & \text{if } \mathrm{p} \neq {}^1\mathrm{H} . \end{cases} \quad (3.45)$$

The variable χ is conveniently defined in terms of the kinetic energy per nucleon of the incident particle

$$\chi(E) = \frac{E - m_{A_i} c^2}{A \left(2 m_{\pi^0} c^2 + \frac{m_{\pi^0}^2 c^2}{2 m_p} \right)} , \quad (3.46)$$

where σ_{ine}^{pp} as in eq. **??** and $\chi_0 \equiv x(1 \text{ PeV})$.

Nucleus-nucleus interactions are usually treated by employing event generators, which are libraries that models a given particle interaction based on their initial state, accounting for the stochasticity of the process at hand. Some widely used event generators include PYTHIA[4] [72, 73], HERWIG [74–76], and Sherpa [77], among others. For higher energy studies, in particular the interaction of CRs with air, commonly used hadronic interaction codes are EPOS [78], QGSJet [79–81], and Sibyll [82, 83]. Note, however, that at ultra-high energys (UHEs), these generators are limited by the availability (or actually lack thereof) of accelerator data, since they operate at much higher energies than what current accelerators can reach.

For astrophysical applications, hadronuclear interactions are usually parametrised based on simulations. Common parametrisations includes those from refs. [66, 67, 84], some of which are also shown in fig. 3.6. One can argue that considering all other astrophysical uncertainties, the parametrisations provide an adequate approximation. However, recent simulation-based studies challenge this assertion [85].

3.6 Energy-loss processes

3.6.1 Cosmological adiabatic losses

Energy losses occur for all particles, due to the adiabatic expansion of the Universe. The change in redshift ($\mathrm{d}z$) corresponding to an infinitesimally small distance $\mathrm{d}\ell$ is described by the equation:

$$\mathrm{d}z = \frac{H_0}{c}\sqrt{\Omega_\Lambda + \Omega_m(1+z)^3}\,\mathrm{d}\ell\;.\tag{3.47}$$

Here, H_0 is the current Hubble parameter, approximately $67.3 \text{ km s}^{-1}\text{ Mpc}^{-1}$, and Ω_m and Ω_Λ stand at about 0.3147 and 0.6853 respectively, representing the matter and dark-energy densities within the flat ΛCDM model, as per references [86]. It is worth noting that eq. 3.47 would include an additional term accounting for radiation, although it is only relevant during the very early stages of the universe's life ($z \gtrsim 1000$).

Ultimately, the energy lost by a particle with an initial energy E_0, as measured at the source, relates to the observed energy (E) as follows:

$$E = \frac{E_0}{1+z}\;.\tag{3.48}$$

3.7 Particle mixing

Processes other than interactions and decays that change the nature of a particle also exist. Within a quantum-mechanical framework, they are usually described by a mixing of some

---
[4]See ref. [71] for a historical overview of this widely-used event generator.

intrinsic eigenstates[5] of a family of particles ($\mathfrak{X}$), which results in propagation eigenstates[6] (X). This notion can be mathematically expressed as

$$
\begin{pmatrix} X_1 \\ \vdots \\ X_n \end{pmatrix} = \begin{pmatrix} U_{11} & \ldots & U_{1n} \\ \vdots & \ddots & \vdots \\ U_{n1} & \ldots & U_{nn} \end{pmatrix} \begin{pmatrix} \mathfrak{X}_1 \\ \vdots \\ \mathfrak{X}_n \end{pmatrix} , \tag{3.49}
$$

where X_i refers to the particle being observed. Here U_{ij} are elements of U, the **mixing matrix**.

If U is diagonal, then there is no *mixing* between states. In this case, the intrinsic states of the particles are exactly equal to the propagation eigenstates. However, if there are non-vanishing off-diagonal elements, the corresponding states will mix among themselves.

The intrinsic eigenstates, by definition, are the free (i.e., in the absence of any potentials) particle solutions to the wave equation, and thus can be written as

$$
|X_i(t)\rangle = |X_i\rangle \exp\left[i\left(\vec{p}_i \cdot \vec{x} - E_i t\right)\right] , \tag{3.50}
$$

where $\vec{p}_i$ and E_i denote the momentum and energy of particle X_i, respectively.

The mixing of states is described by the Schrödinger equation:

$$
i\hbar \frac{d|\psi\rangle}{dt} = H|\psi\rangle , \tag{3.51}
$$

wherein H is the Hamiltonian of the system and

$$
|\psi\rangle = \sum_{j=1}^{n} a_j |X_j\rangle , \tag{3.52}
$$

for arbitrary constants c_j satistfying the condition $\sum_j |a_j|^2 = 1$.

The time-evolution operator, assuming that the H is time-independent, is defined as

$$
U(t) = \exp\left(-\frac{i}{\hbar} H t\right) . \tag{3.53}
$$

The connection between intrinsic and propagation eigenstates through the unitary ($U^\dagger U = \mathbb{I}$) matrix U is

$$
|X_i\rangle = \sum_{j=1}^{n} U_{ij} |\mathfrak{X}_j\rangle . \tag{3.54}
$$

---

[5]This terminology is not found elsewhere in the literature. In principle, there is no such thing as an *intrinsic eigenstate*, since any basis can be chosen to describe the same phenomenon. Depending on one's philosophical inclinations, what I am calling intrinsic eigenstates can have an *ontological* meaning, with direct correspondence with real-world entities. However, for the purposes of this discussion it suffices to understand these states as the eigenstates of the free Hamiltonian.

[6]Once again, I make up a nomenclature that is not usually found in the literature, *propagation eigenstate*. This refers to the states represented in a basis convenient for describing what is actually observed after the particle, which is a quantum superposition of states, travelled a certain distance.

Conversely, since U is unitary,

$$|\mathfrak{X}_i\rangle = \sum_{j=1}^{n} U_{ij}^* |X_j\rangle .$$

(3.55)

The probability (P_{X_i}) that a state X_i will be detected after the particle travelled a distance L is simply the sum of the probabilities of each component ending up as X_i:

$$P_{X_i}(L) = \sum_{j=1}^{n} \left| \langle X_i | \mathfrak{X}_j \rangle \right|^2 .$$

(3.56)

The general form given by eq. 3.49 can be applied to many problems, the most notorius of which is neutrino oscillations, described in §3.7.1.

3.7.1 Neutrino oscillations

Neutrinos are detected in what is called *flavour states* — the electron (ν_e), the muon (ν_μ) and the ν_τ neutrinos — the **flavour eigenstates**, which correspond to what had been previously been called propagation eigenstates. However, they are a superposition of intrinsic eigenstates, which for neutrinos are *mass eigenstates*[7].

The original idea of neutrino oscillations dates back to the late 1950s, building on the work of B. Pontecorvo [87]. The underlying theory of oscillations was further developed in the following decade by others [88, 89]. Only towards the end of the 20th century has this phenomenon been unambiguously confirmed through observations of solar neutrinos [90, 91].

Let ν represent the flavour state of a neutrino, and υ its mass state. If propagation is in vacuum, the mixing matrix (U) has the general form

$$U = \begin{pmatrix} U_{e1} & U_{e2} & U_{e3} \\ U_{\mu1} & U_{\mu2} & U_{\mu3} \\ U_{e\tau1} & U_{\tau2} & U_{\tau3} \end{pmatrix} ,$$

(3.57)

where U_{e1} refers to the mixing between the mass eigenstate 1 and the flavour state corresponding to the electron neutrino (e), and similarly for the other terms. U is the so-called Pontecorvo-Maki-Nakagawa-Sakata (PMNS) matrix, given by

$$U = \begin{pmatrix} c_{12}c_{13} & s_{12}c_{13} & s_{13}e^{-i\delta} \\ -s_{12}c_{23} - c_{12}s_{23}s_{13}e^{i\delta} & c_{12}c_{23} - s_{12}s_{23}s_{13}e^{i\delta} & s_{23}c_{13} \\ s_{12}s_{23} - c12c_{23}s_{13}e^{i\delta} & -c_{12}s_{23} - s12c_{23}s_{13}e^{i\delta} & c_{23}c_{13} \end{pmatrix} \begin{pmatrix} e^{i\alpha_1/2} & 0 & 0 \\ 0 & e^{i\alpha_2/2} & 0 \\ 0 & 0 & 1 \end{pmatrix} ,$$

(3.58)

wherein $c_{ij} \equiv \cos\theta_{ij}$ and $s_{ij} \equiv \sin\theta_{ij}$, and α_i in the right-most matrix is related to whether neutrinos are Dirac or Majorana particles.

---

[7]Sometimes the mass eigenstates are referred to as *physical eigenstates*. I prefer to avoid such terminology, due to the philosophical implications of the word 'physical'. There is no guarantee that the mass eigenstates have direct correspondence to what really exists in reality. In fact, what we call neutrinos might simply be a manifestation of other yet-unknown phenomenon which, in this view, would be even more "physical".

Eq. 3.58, together with eq. 3.56, allow the calculation of oscillation probabilities, which is used to infer neutrino states after propagating in the universe. Note, however, that this assumes propagation in vacuum. While this assumption is adequate for many applications, this is not always the case. For that the Hamiltonian that goes into the Schrödinger equation (eq. 3.51) would change, making the treatment more complicated and often requiring advanced computational methods for the solution.

3.8 Exercises

3.1 The relativistic Larmor formula for the power radiated by an accelerated charge is:

$$\frac{\mathrm{d}E}{\mathrm{d}t} = -\frac{q^2\gamma^4}{6\pi\varepsilon_0 c^3}\left(\gamma^2|a_\parallel|^2 + |a_\perp|^2\right) .$$

(a) Derive this equation. (*Hint:* Use Liénard-Wiechert potentials.)

(b) Compute the power radiated per solid angle element.

(c) If an observer sees synchrotron radiation emitted by a particle at an angle θ_{obs}, how does this relatd to the synchrotron power measured by another observer at an angle $\theta'_{\mathrm{obs}} > \theta_{\mathrm{obs}}$? Discuss.

(d) Demonstrate (mathematically) that the synchrotron spectrum for relativistic particles is strongly beamed in the forward direction. Explain the underlying reasoning.

3.2 Muons are abundantly produced in astrophysical environments through the decay of charged pions, being the most important channel for neutrino production. Their main decay channel is:

$$\mu^- \to e^- + \bar{\nu}_e + \nu_\mu .$$
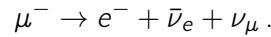
Their lifetime in their own rest frame is approximately $\tau_\mu \approx 2.2\ \mu$s, and their mass is $m_\mu \approx 106\ \mathrm{MeV}/c^2$.

(a) Estimate the amount of energy that a muon with Lorentz factor $\gamma_\mu = 10^6$, measured in the lab frame, will radiate via synchrotron emission, within a time interval of $2.2\ \mu$s. Do this calculation for a galaxy cluster ($B \sim 0.1$ nT) and a the surroundings of a GRB ($B \sim 1$ kT).

(b) Compute the maximum energy (E_e^{max}) the electron can take away from the muon. Explain your reasoning and assumptions made.

(c) Suppose the muon decays within τ_μ in its own rest frame. How much time will it have lived according to the observer of item (a)?

(d) The characteristic synchrotron cooling time is defined as

$$\tau_{\mathrm{sync}} = E\left|\frac{\mathrm{d}E}{\mathrm{d}t}\right|^{-1} .$$

Compare this quantity, τ_{sync}, with the lifetime of the muon estimated in (b). What can you infer from this comparison? Is muon synchrotron an important channel for the energy loss of muons in astrophysical environments?

3.3 Suppose two protons collide and produce other particles, while still remaining protons:

$$p + p \to p + p + \dots ,$$
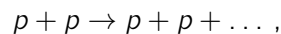
where the ellipsis ('...') refer to the other particles produced. (a) What is the simplest way

to produce anti-protons out of this collision? Write down the reaction.

(b) Compute the minimum squared centre-of-mass energy (s) required for this reaction to be possible.

High-energy protons travelling in the interstellar medium produce, among other particles, co-pious amounts of anti-protons. (c) Suppose proton-proton interactions is the main channel for anti-proton production. Do you think that the spectrum of anti-protons is the same as that of protons? Explain your reasoning.

3.4   Some collisions between protons and photons produce roughly the same amount of π^0, π^+, and π^- mesons. This is due to the characteristic isospin symmetry of the strong interaction.

Suppose the main decay channels of pions are:

$$\pi^0 \rightarrow \gamma + \gamma \,,$$

$$\pi^+ \rightarrow \mu^+ + \nu_\mu \rightarrow e^- + \bar{\nu}_e + \nu_\mu + \bar{\nu}_\mu \,,$$

$$\pi^- \rightarrow \mu^- + \bar{\nu}_\mu \rightarrow e^+ + \nu_e + \bar{\nu}_\mu + \nu_\mu \,.$$

Compute the ratio of photons to neutrinos of each species.

3.5   Consider the interaction between a cosmic-ray proton and a cosmological photon. Suppose this interaction produced a neutral pion, whose decay is given by

$$\pi^0 \rightarrow \gamma + \gamma \,.$$

a. Is it possible for the two photons to have different energies? Discuss in detail.

b. Compute the energy of each photon in the rest frame of the pion.

c. Suppose the pion has an energy E_{π^0} in the laboratory frame.

3.6   Consider the reaction $^2_4\text{He} + \gamma_{\text{bg}} \rightarrow ^1_3\text{H} + p$.

(a) Calculate the minimum squared centre-of-mass energy (s_{min}) for this process to happen.

(b) Based on this result, estimate the minimum energy of the helium nucleus (E_{min}), in the lab frame, considering a typical photon from the CMB ($\varepsilon_{\text{CMB}} \sim 0.5$ meV) and another one from the EBL ($\varepsilon_{\text{EBL}} \sim 1$ eV).

Astroparticle Propagation

Astroparticles detected at Earth are not necessarily the same as those that left the sources. A lot can happen to them as they traverse cosmic expanses. This chapter provides the theoretical framework for describing the motion of cosmic messengers after they are produced (see §1 for a discussion on acceleration mechanisms), until they reach Earth. It discusses the possible interactions of these particles with matter and radiation fields pervading the universe, whose theoretical basis is provided in §3. It also touches upon how these particles are transported through putative cosmic magnetic fields along the way, which can alter their trajectories (see §2).

4.1 Propagation models: ingredients

4.1.1 Radiation fields

The universe is permeated with radiation covering a wide frequency range of the electromagnetic spectrum. This radiation may be the integrated diffuse signal resulting from structure formation processes, like the EBL and the cosmic radio background (CRB), or a relic of some primeval process, as the CMB. These three backgrounds are the most important ones when it comes to modelling the propagation of astroparticles over cosmological distances.

A general overview of the energy density of the different backgrounds is shown in figure 4.1. Note that, while this figure refers to redshift $z = 0$, these models can differ considerably at higher redshifts.

There are other radiation fields that may impact particle propagation. For instance, in the Milky Way the interstellar radiation field (ISRF) plays an important role for the propagation of Galactic cosmic rays (GCRs) and very energetic photons [98].

4.1.1.1 Cosmic Microwave Background (CMB)

The CMB is a blackbody of temperature $T_{cmb} \approx 2.73$ K [86], with energy density given by

$$\frac{\mathrm{d}n(\varepsilon, z)}{\mathrm{d}\varepsilon} = \frac{\varepsilon^2}{\pi^2 c^3 \hbar^2} \left[\exp\left(\frac{\varepsilon}{k_B T_{CMB}} \right) - 1 \right]^{-1} (1 + z)^2 , \qquad (4.1)$$
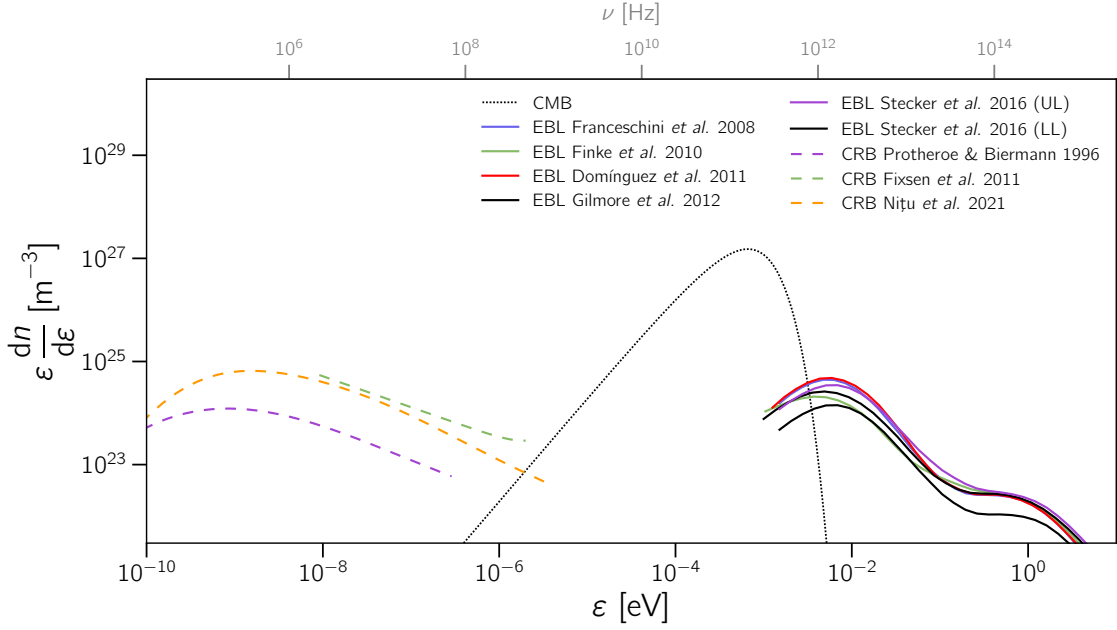
Figure 4.1: Number density of photons at $z = 0$ for different backgrounds: CMB (dotted), EBL (solid) [92–94], and CRB (dashed lines) [95, 96]. Different colours correspond to different models. The shaded band represent the uncertainties of the indicated model. Figure adapted from ref. [97].

where k_B is Boltzmann's constant, T_{CMB} the CMB temperature, and ε the photon energy. The energy density of CMB photons today is $\simeq 4 \times 10^8$ m^{-3} (see fig. 4.1).

4.1.1.2 Extragalactic Background Light (EBL)

The extragalactic background light (EBL) is a diffuse flux of radiation produced during the formation of structures along the universe's history, most of which is due to star formation [99–101]. The peaks of the EBL distribution are mostly in the infrared and optical bands, with a tail extending to the ultraviolet, usually attributed to photons emitted by hot objects being scattered by dust [102–104]. Several models exists for the EBL, some are purely empirical (for example, [93, 105–108]), whereas others are semi-analytical (e.g. [92, 94]). They tend to generally agree on the spectrum at low redshifts, but there is considerable discrepancy at higher redshifts [93].

4.1.1.3 Cosmic Radio Background (CRB)

The cosmic radio background (CRB) can play an important role in the propagation of astroparticles depending on their energy, although it can be ignored in many types of study. It is mostly dominated by radio emission from normal, radio, and starburst galaxies [109, 110]. CRB models commonly used to study the propagation of UHE particles include the ones from refds. [95, 96].

4.1.2 Magnetic fields

4.2 Interaction length

Now the problem at hand consists in finding the probability that a (projectile) particle will interact with target particles, after a given distanc. Classically, considering a collection of target particles at rest in the laboratory frame, this probability is related to the notion of cross section (σ), described in §3.1.2, which takes into account the amount of "free space" in a target that would allow for an incident particle to cross. Therefore, the classical notion is purely geometrical, similar to what was originally described by Ernest Rutherford in his well-known 1911 experiment [111].

The classical notion of cross section has to be abandoned when treating quantum scattering. Moreover, particles might not all be static, which makes the treatment more intricate. Henceforth I will employ this broader definition, despite the fact that I will present a seemingly "semi-classical" approach to formulate the problem and obtain a general solution.

Suppose a medium composed by an admixture of two types of particles, 1 and 2, with number densities $n_1(\vec{p}_1)$ and $n_2(\vec{p}_2)$. The number densities n_1 and n_2 are calculated in this arbitrary frame, which transforms to their own rest frame, indicated by the superscript o, as follows:

$$n_j(\vec{p}_j) = \gamma_j n_j^{\mathrm{o}}(\vec{p}_j) \,, \tag{4.2}$$

for $j = 1, 2$, referring to each of the particle species, where γ_j is the corresponding Lorentz factor of the particle in the arbitrary frame.

The number of interacting particles ($\mathrm{d}N$) per unit time ($\mathrm{d}t$) and volume ($\mathrm{d}V$), is given by

$$\boxed{\frac{\mathrm{d}^4 N}{\mathrm{d}V \mathrm{d}t} = \sigma(s) \, c\beta_{\mathrm{rel}}(P_1, P_2) \, n_1(\vec{p}_1) \, n_2(\vec{p}_2) \,,} \tag{4.3}$$

with $c\beta_{\mathrm{rel}}(P_1, P_2)$ being the relative velocity, given by

$$\beta_{\mathrm{rel}}(P_1, P_2) = \sqrt{1 - \frac{(m_1 m_2 c^2)^2}{(P_1 \cdot P_2)^2}} \,, \tag{4.4}$$

which is more conveniently expressed in the form [112]:

$$\beta_{\mathrm{rel}}\left(\vec{\beta}_1, \vec{\beta}_2\right) = \begin{cases} 1 & \text{if } \left(|\vec{\beta}_1| = 1\right) \vee \left(|\vec{\beta}_2| = 1\right) \,, \\[2mm] \dfrac{\sqrt{|\vec{\beta}_1 - \vec{\beta}_2|^2 - |\vec{\beta}_1 \times \vec{\beta}_2|^2}}{1 - \vec{\beta}_1 \cdot \vec{\beta}_2} & \text{otherwise} \,. \end{cases} \tag{4.5}$$

> **Exercise.** Show that the number of particles per unit volume per unit time,
>
> $$\frac{\mathrm{d}^4 N}{\mathrm{d}V \mathrm{d}t},$$
>
> defined in eq. 4.2, is relativistic invariant.

The Lorentz factor in the direction of relative motion between the two particles (γ_{rel}) can be easily computed from the four-momenta of the particles or the relative velocity [113]:

$$\gamma_{\text{rel}} = \frac{1}{\sqrt{1 - \beta_{\text{rel}}}} = \frac{P_1 \cdot P_2}{m_1 m_2 c^2} = \gamma_1 \gamma_2 \left(1 - \vec{\beta}_1 \cdot \vec{\beta}_2\right), \tag{4.6}$$

where γ_1 and γ_2 are the Lorentz factors of the particles 1 and 2 in the arbitrary reference frame considered here. Now it is possible to choose the rest frame of one of the particles[1], say particle 1, to proceed with the calculations. In this case, only particle species 1 transforms, according to the relative Lorentz factor given by eq. 4.6. As a consequence, eq. 4.3 can be rewritten as

$$\frac{\mathrm{d}^4 N}{\mathrm{d}V \mathrm{d}t} = \sigma(s)\, c \beta_{\text{rel}}(P_1, P_2)\, (1 - \vec{\beta}_1 \cdot \vec{\beta}_2)\, n_1(\vec{p}_1)\, n_2(\vec{p}_2). \tag{4.7}$$

If there are N_0 particles of type 1, it is possible to define the scattering rate (Γ) and the mean free path (λ) from eq. 4.7:

$$\Gamma \equiv \frac{1}{N_0} \frac{\mathrm{d}N}{\mathrm{d}t} \quad \Rightarrow \quad \lambda = \frac{\beta_1 c}{\Gamma}. \tag{4.8}$$

4.2.1 Interaction with isotropic photons

A problem of great astrophysical significance is the interaction with photons, which is the dominant process for high-energy particles travelling large distances. Some of these processes were described in §3. Given the omnipresence of photons in the universe, such as the CMB and the EBL (see details in §4.1.1), it is useful to consider the interaction of a particle of type 1 with a target distribution of isotropic photons.

In this case, the relative velocity is $\beta_{\text{rel}} = 1$. The indices 1 and 2, which refer to the projectile particle the photon, respectively, will be dropped, and the energy of the photon will be denoted ε. Therefore, from these considerations, it is possible to compute the **mean free path** (λ) for this class of processes:

$$\lambda^{-1}(E) = \frac{1}{2\beta_1} \int\limits_{\varepsilon_{\text{min}}}^{\varepsilon_{\text{max}}} \int\limits_{-1}^{+1} \mathrm{d}\varepsilon\, \mathrm{d}\cos\theta\, \sigma(s)\, (1 - \beta_1 \cos\theta)\, \frac{\mathrm{d}n(\varepsilon)}{\mathrm{d}\varepsilon}. \tag{4.9}$$

Eq. 4.10 seems to be a general expression for the mean free path of a particle of type 1 interacting with a target distribution of particles of photons. However, the limits of integration

---

[1] If this particle is a photon, then there is no way to define a rest frame. However, it follows from eq. 4.4 that $\beta_{\text{rel}} = 1$, and the treatment would be even simpler.

ε_{min} and ε_{max} are not specified. It would be reasonable to presume that the limits are 0 and ∞, respectively. However, this is not the case. Certain interactions can only happen if the energy of the photon is within certain limits. There are **interaction thresholds** that ensure that there is sufficient energy and momentum for the interaction to take place and produce the final-state particles. The upper threshold, ε_{max}, would likely break at some extremely high energy scale like the Planck energy (but there are no such energetic backgrounds). The lower threshold, ε_{min}, is the trickier one, since it depends on the kinematics of the process at hand.

Eq. 4.10 can be written in a variety of ways, depending on the specific process being considered. Another convenient form is:

$$\lambda^{-1}(E) = \frac{1}{8\beta E^2} \int\limits_{\varepsilon_{min}}^{\varepsilon_{max}} \int\limits_{s_{min}}^{s_{max}} d\varepsilon \, ds \, \frac{1}{\varepsilon^2}(s - m^2 c^4)\frac{dn(\varepsilon)}{d\varepsilon} \, , \tag{4.10}$$

where m denotes the mass of the projectile particle, and s refers to the squared centre of momentum (CM) energy. Here $\varepsilon_{min} = \varepsilon_{min}(E)$, $\varepsilon_{max} \to \infty$, $s_{max} = s_{max}(E, \varepsilon)$.

> **Exercise.** Derive eq. 4.10 from eq. 4.9.

4.3 Optical depth

Consider an astrophysical object located at a distance D_s, corresponding to a redshift z_s, emits particles of a given type with energy E_s, as measured at the source. Let $\Phi_s(E_s)$ denote this flux. After propagation, a fraction of these particles might be absorbed through the interactions, never reaching Earth. Due to the expansion of the universe, discussed in §3.6.1, the energy of the particles at the source (E_s) will be different from the energy of the particles observed at Earth (E), through eq. 4.11:

$$E_s = E\,(1 + z_s) \, . \tag{4.11}$$

The flux of particles of energy E reaching Earth ($\Phi_{obs}(E)$) is given by:

$$\Phi_{obs}(E) = \Phi_s(E_s) \exp\left(-\tau(E, z_s)\right) \, . \tag{4.12}$$

where $\tau_{abs}(E, z)$ is the **optical depth**, which is essentially the distance-integrated inverse mean free path:

$$\tau_{abs}(E) = \int\limits_{0}^{D_s} d\ell \, \lambda^{-1}(E) \, , \tag{4.13}$$

where D_s refers to the distance of the origin of the particle to the observer. This equation is a bit misleading, since there is no guarantee that the background photon distribution remains the same over time. Moreover, for extragalactic studies, the expansion of the universe might

become an issue. Therefore, it is useful to use instead the redshift-dependent (see §3.6.1) photon density $\left(\frac{\mathrm{d}n(\varepsilon,z)}{\mathrm{d}\varepsilon}\right)$ and mean free path $(\lambda(E) \to \lambda(E,z))$, and perform a change of variables in the equation above. This leads to the following expression:

$$\tau_{\mathrm{abs}}(E, z) = \int\limits_{0}^{z_{\mathrm{s}}} \mathrm{d}z \; \lambda^{-1}(E, z)\frac{\mathrm{d}\ell}{\mathrm{d}z} , \qquad (4.14)$$

where z_{s} is the redshift of origin of the particle.

The optical depth is a crucial quantity in high-energy astrophysics. One example is the attenuation of high-energy gamma rays as they travel through the universe, and to estimate the distance to the source of these photons. One example is shown in fig. 4.2, where the optical depth for gamma rays is shown as a function of energy for different redshifts and different models of the EBL.
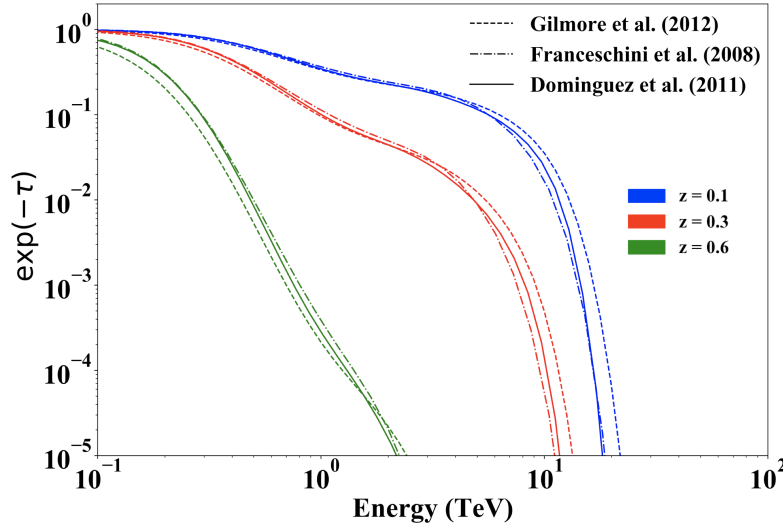

Figure 4.2: Flux attenuation factor $(\exp(-\tau_{\mathrm{abs}}))$ for different redshifts, considering different EBL models. Figure taken from ref. [97].

A remarkable feature visibile in fig. 4.2 is the strong suppression at energies above several TeV. That imposes an effective horizon for gamma-ray astronomy, beyond which the number of expected gamma rays detectable at Earth would drop to virtually zero, due to interactions with the EBL.

4.4 Exercises

4.1 Consider an isotropic cosmological monochromatic photon background described by

$$\frac{\mathrm{d}n}{\mathrm{d}\varepsilon}(\varepsilon, z) = \frac{3}{4\pi R_{\mathrm{H}}^3 \varepsilon_0} \delta(\varepsilon - \varepsilon_0)(1 + z)^2,$$

where δ denotes the Dirac delta function, and R_{H} is the (co-moving) Hubble radius and ε_0 is characteristic photon energy of this background, at a given reshift z.

(a) If a high-energy particle X, whose interaction with photons has a constant cross section $\sigma_{X\gamma} = \sigma_0$, propagates through this photon background, how far would it travel, on average?

(b) Suppose the source of this particle is located at redshift z_{s}, with $z_{\mathrm{s}} \ll 1$. Calculate the optical depth in this case, using the following approximation:

$$\frac{\mathrm{d}z}{\mathrm{d}t} = -H_0 \sqrt{\Omega_\Lambda},$$

where Ω_Λ is the density of dark energy at present time.

(c) Draw a sketch of what you expect the flux $(\Phi_X(E))$ will look like, as seen from Earth, for three sources located at $z_1 < z_2 < z_3$, for $z_i \ll 1$.

4.2 Compute the threshold squared centre-of-mass energy (s) for Breit-Wheeler pair production in the collision of two photons with energies E and ε.

Bibliography

[1] Fly's Eye Collaboration, "Detection of a cosmic ray with measured energy well beyond the expected spectral cutoff due to cosmic microwave radiation", The Astrophysical Journal **441**, 144–150 (1995).

[2] Telescope Array Collaboration, "An extremely energetic cosmic ray observed by a surface detector array", Science **382**, 903–907 (2023).

[3] Telescope Array Collaboration, "Constraints on the diffuse photon flux with energies above 10^{18} eV using the surface detector of the Telescope Array experiment", Astroparticle Physics **110**, 8–14 (2019).

[4] Pierre Auger Collaboration, "A search for photons with energies above 2×10^{17} eV using hybrid data from the low-energy extensions of the Pierre Auger Observatory", The Astrophysical Journal **933**, 125, 125 (2022).

[5] Pierre Auger Collaboration, "Cosmological implications of photon-flux upper limits at ultrahigh energies in scenarios of Planckian-interacting massive particles for dark matter", Physical Review D **107**, 042002, 042002 (2023).

[6] E. Fermi, "On the Origin of the Cosmic Radiation", Physical Review **75**, 1169–1174 (1949).

[7] M. S. Longair, *High Energy Astrophysics*, 3rd (Cambridge University Press, Cambridge, United Kingdom, 2011).

[8] A. R. Bell, "The acceleration of cosmic rays in shock fronts - I.", Monthly Notices of the Royal Astronomical Society **182**, 147–156 (1978).

[9] G. F. Krymskii, "A regular mechanism for the acceleration of charged particles on the front of a shock wave", Soviet Physics Doklady **22**, 327 (1977).

[10] W. I. Axford, E. Leer, and G. Skadron, "The acceleration of cosmic rays by shock waves", in Proceedings of the 15th international cosmic ray conference, Vol. 11, International Cosmic Ray Conference (1977), pp. 132–137.

[11] R. D. Blandford and J. P. Ostriker, "Particle acceleration by astrophysical shocks", The Astrophysical Journal Letters **221**, L29–L32 (1978).

[12] A. R. Bell, "The acceleration of cosmic rays in shock fronts - II.", Monthly Notices of the Royal Astronomical Society **182**, 443–455 (1978).

[13] L. O. Drury, "An introduction to the theory of diffusive shock acceleration of energetic particles in tenuous plasmas", Reports on Progress in Physics **46**, 973–1027 (1983).

[14] M. Bietenholz, "Supernova VLBI", in The role of vlbi in the golden age for radio astronomy, Vol. 9 (January 2008), p. 64.

[15] R. Penrose, "Gravitational Collapse: the Role of General Relativity", Nuovo Cimento Rivista Serie **1**, 252 (1969).

[16] K. V. Ptitsyna and S. V. Troitsky, "Physical conditions in potential accelerators of ultra-high-energy cosmic rays: updated Hillas plot and radiation-loss constraints", Physics Uspekhi **53**, 691–701 (2010).

[17] A. M. Hillas, "The Origin of Ultra-High-Energy Cosmic Rays", Annual Reviews of Astronomy and Astrophysics **22**, 425–444 (1984).

[18] R. Alves Batista et al., "White paper and roadmap for quantum gravity phenomenology in the multi-messenger era", Classical and Quantum Gravity **42**, 032001, 032001 (2025).

[19] R. V. E. Lovelace, "Dynamo model of double radio sources", Nature **262**, 649–652 (1976).

[20] G. I. Taylor, "Diffusion by Continuous Movements", Proceedings of the London Mathematical Society **s2-20**, 196–212 (1922).

[21] M. S. Green, "Brownian Motion in a Gas of Noninteracting Molecules", The Journal of Chemical Physics **19**, 1036–1046 (1951).

[22] R. Kubo, "Statistical-Mechanical Theory of Irreversible Processes. I", Journal of the Physical Society of Japan **12**, 570–586 (1957).

[23] A. D. Fokker, "Die mittlere Energie rotierender elektrischer Dipole im Strahlungsfeld", Annalen der Physik **348**, 810–820 (1914).

[24] M. Planck, "Über einen Satz der statistischen Dynamik und seine Erweiterung in der Quantentheorie", Sitzungsberichte der Preussischen Akademie der Wissenschaften zu Berlin **24**, 324–341.

[25] A. Kolmogorov, "Über die analytischen methoden in der wahrscheinlichkeitsrechnung", Mathematische Annalen **104**, 415–458 (1931).

[26] W. H. Matthaeus, G. Qin, J. W. Bieber, and G. P. Zank, "Nonlinear Collisionless Perpendicular Diffusion of Charged Particles", The Astrophysical Journal Letters **590**, L53–L56 (2003).

[27] A. Lazarian and H. Yan, "Superdiffusion of Cosmic Rays: Implications for Cosmic Ray Acceleration", The Astrophysical Journal **784**, 38, 38 (2014).

[28] T. K. Gaisser, R. Engel, and E. Resconi, *Cosmic rays and particle physics* (Cambridge University Press, 2016).

[29] V. L. Ginzburg and S. I. Syrovatskii, *The origin of cosmic rays* (Pergamon Press, 1969).

[30] R. Ramaty and R. E. Lingenfelter, "Cosmic-Ray Deuterium and HELIUM-3 of Secondary Origin and the Residual Modulation of Cosmic Rays", The Astrophysical Journal **155**, 587 (1969).

[31] G. Gloeckler and J. R. Jokipii, "Physical Basis of the Transport and Composition of Cosmic Rays in the Galaxy", Physical Review Letters **22**, 1448–1453 (1969).

[32] J. Davis L., "On the diffusion of cosmic rays in the galaxy", in International cosmic ray conference, Vol. 3, International Cosmic Ray Conference (January 1960), p. 220.

[33] C. F. Jones et al., "The Leaky Box: An Idea Whose Time is Up?", in International cosmic ray conference, Vol. 3, International Cosmic Ray Conference (January 1990), p. 333.

[34] AMS Collaboration, "Precision Measurement of the Boron to Carbon Flux Ratio in Cosmic Rays from 1.9 GV to 2.6 TV with the Alpha Magnetic Spectrometer on the International Space Station", Physical Review Letters **117**, 231102, 231102 (2016).

[35] A. Kolmogorov, "The Local Structure of Turbulence in Incompressible Viscous Fluid for Very Large Reynolds' Numbers", Akademiia Nauk SSSR Doklady **30**, 301–305 (1941).

[36] J. Larmor, "LXIII. On the theory of the magnetic influence on spectra; and on the radiation from moving ions", Philosophical Magazine **44**, 503–512 (1897).

[37] R. Alves Batista and A. Saveliev, "The Gamma-Ray Window to Intergalactic Magnetism", Universe **7**, 223 (2021).

[38] G. Breit and J. A. Wheeler, "Collision of Two Light Quanta", Physical Review **46**, 1087–1091 (1934).

[39] R. Alves Batista, "On the cosmological propagation of high energy particles in magnetic fields", PhD thesis (Universität Hamburg, April 2015).

[40] A. H. Compton, "A Quantum Theory of the Scattering of X-rays by Light Elements", Physical Review **21**, 483–502 (1923).

[41] R. H. Stuewer, *The Compton effect. Turning points in physics.* (Science History Publications, 1975).

[42] S. Lee, "Propagation of extragalactic high energy cosmic and γ rays", Physical Review D **58**, 043004, 043004 (1998).

[43] A. A. Zdziarski, "Saturated Pair-Photon Cascades on Isotropic Background Photons", The Astrophysical Journal **335**, 786 (1988).

[44] H. Bethe and W. Heitler, "On the Stopping of Fast Particles and on the Creation of Positive Electrons", Proceedings of the Royal Society of London Series A **146**, 83–112 (1934).

[45] V. Berezinsky, A. Z. Gazizov, and S. I. Grigorieva, "Dip in UHECR spectrum as signature of proton interaction with CMB", Physics Letters B **612**, 147–153 (2005).

[46] A. Coleman et al., "Ultra high energy cosmic rays The intersection of the Cosmic and Energy Frontiers", Astroparticle Physics **147**, 102794, 102794 (2023).

[47] G. T. Zatsepin and V. A. Kuz'min, "Upper Limit of the Spectrum of Cosmic Rays", Soviet Journal of Experimental and Theoretical Physics Letters **4**, 78 (1966).

[48] K. Greisen, "End to the Cosmic-Ray Spectrum?", Physical Review Letters **16**, 748–750 (1966).

[49] F. W. Stecker and M. H. Salamon, "Photodisintegration of Ultra-High-Energy Cosmic Rays: A New Determination", The Astrophysical Journal **512**, 521–526 (1999).

[50] L. Morejon, A. Fedynitch, D. Boncioli, D. Biehl, and W. Winter, "Improved photomeson model for interactions of cosmic ray nuclei", Journal of Cosmology and Astroparticle Physics **2019**, 007, 007 (2019).

[51] E. Khan et al., "Photodisintegration of ultra-high-energy cosmic rays revisited", Astroparticle Physics **23**, 191–201 (2005).

[52] R. Alves Batista, D. Boncioli, A. di Matteo, A. van Vliet, and D. Walz, "Effects of uncertainties in simulations of extragalactic UHECR propagation, using CRPropa and SimProp", Journal of Cosmology and Astroparticle Physics **10**, 063, 063 (2015).

[53] J. F. Soriano, L. A. Anchordoqui, and D. F. Torres, "Photo-disintegration of ^{4}He on the cosmic microwave background is less severe than earlier thought", Physical Review D **98**, 043001, 043001 (2018).

[54] R. Alves Batista, D. Boncioli, A. di Matteo, and A. van Vliet, "Secondary neutrino and gamma-ray fluxes from SimProp and CRPropa", Journal of Cosmology and Astroparticle Physics **5**, 006, 006 (2019).

[55] LHCf Collaboration, "Measurement of forward neutral pion transverse momentum spectra for $\sqrt{s}$=7 TeV proton-proton collisions at the LHC", Physical Review D **86**, 092001, 092001 (2012).

[56] TOTEM Collaboration, "Luminosity-Independent Measurement of the Proton-Proton Total Cross Section at $\sqrt{s}$ = 8 TeV", Physical Review Letters **111**, 012001, 012001 (2013).

[57] TOTEM Collaboration, "Evidence for non-exponential elastic proton-proton differential cross-section at low $|t|$ and $\sqrt{s}$=8 TeV by TOTEM", Nuclear Physics B **899**, 527–546 (2015).

[58] ATLAS Collaboration, "Measurement of the Inelastic Proton-Proton Cross Section at $\sqrt{s}$=13 TeV with the ATLAS Detector at the LHC", Physical Review Letters **117**, 182002, 182002 (2016).

[59] ATLAS Collaboration, "Measurement of the total cross section from elastic scattering in pp collisions at $\sqrt{s}$=8 TeV with the ATLAS detector", Physics Letters B **761**, 158–178 (2016).

[60] LHCf Collaboration, "Measurement of forward photon production cross-section in proton-proton collisions at $\sqrt{s}$=13 TeV with the LHCf detector", Physics Letters B **780**, 233–239 (2018).

[61] STAR Collaboration, "Measurement of the central exclusive production of charged particle pairs in proton-proton collisions at $\sqrt{s}$= 200 GeV with the STAR detector at RHIC", Journal of High Energy Physics **2020**, 178, 178 (2020).

[62] R. M. Baltrusaitis et al., "Total proton-proton cross section at $\sqrt{s}$ = 30 TeV", Physical Review Letters **52**, 1380–1383 (1984).

[63] T. Wibig and D. Sobczynska, "Proton-nucleus cross section at high energies", Journal of Physics G Nuclear Physics **24**, 2037–2047 (1998).

[64] T. Wibig, "Very high energy proton-proton cross section", Physical Review D **79**, 094008, 094008 (2009).

[65] Z. Plebaniak and T. Wibig, "Extrapolation of proton-proton cross section to cosmic ray energies using geometrical model", European Physical Journal Web of Conferences **145**, 13004, 13004 (2017).

[66] S. R. Kelner, F. A. Aharonian, and V. V. Bugayov, "Energy spectra of gamma rays, electrons, and neutrinos produced at proton-proton interactions in the very high energy regime", Physical Review D **74**, 034018, 034018 (2006).

[67] E. Kafexhiu, F. Aharonian, A. M. Taylor, and G. S. Vila, "Parametrization of gamma-ray production cross sections for p p interactions in a broad proton energy range from the kinematic threshold to PeV energies", Physical Review D **90**, 123014, 123014 (2014).

[68] R. J. Glauber and G. Matthiae, "High-energy scattering of protons by nuclei", Nuclear Physics B **21**, 135–157 (1970).

[69] S. Barshay, C. B. Dover, and J. P. Vary, "Nucleus-nucleus cross sections and the validity of the factorization hypothesis at intermediate and high energies", Physical Review C **11**, 360–369 (1975).

[70] L. Sihver, C. H. Tsao, R. Silberberg, T. Kanai, and A. F. Barghouty, "Total reaction and partial cross section calculations in proton-nucleus ($Z\_t \leq 26$) and nucleus-nucleus reactions (Z_p and $Z\_t <= 26$)", Physical Review C **47**, 1225–1236 (1993).

[71] T. Sjöstrand, "The PYTHIA event generator: Past, present and future", Computer Physics Communications **246**, 106910, 106910 (2020).

[72] T. Sjöstrand et al., "High-energy-physics event generation with PYTHIA 6.1", Computer Physics Communications **135**, 238–259 (2001).

[73] C. Bierlich et al., *A comprehensive guide to the physics and usage of PYTHIA 8.3*, tech. rep. (March 2022), arXiv:2203.11601.

[74] M. Bähr et al., "Herwig++ physics and manual", European Physical Journal C **58**, 639–707 (2008).

[75] J. Bellm et al., "Herwig 7.0/Herwig++ 3.0 release note", European Physical Journal C **76**, 196, 196 (2016).

[76] J. Bellm et al., "Herwig 7.2 release note", European Physical Journal C **80**, 452, 452 (2020).

[77] T. Gleisberg et al., "Event generation with SHERPA 1.1", Journal of High Energy Physics **2009**, 007, 007 (2009).

[78] T. Pierog, I. Karpenko, J. M. Katzy, E. Yatsenko, and K. Werner, "EPOS LHC: Test of collective hadronization with data measured at the CERN Large Hadron Collider", Physical Review C **92**, 034906 (2015).

[79] S. Ostapchenko, "QGSJET-II: towards reliable description of very high energy hadronic interactions", Nuclear Physics B Proceedings Supplements **151**, 143–146 (2006).

[80] S. Ostapchenko, "Monte Carlo treatment of hadronic interactions in enhanced Pomeron scheme: QGSJET-II model", Physical Review D **83**, 014018, 014018 (2011).

[81] S. Ostapchenko, "QGSJET-III model: physics and preliminary results", in European physical journal web of conferences, Vol. 208, European Physical Journal Web of Conferences (May 2019), p. 11001.

[82] E.-J. Ahn, R. Engel, T. K. Gaisser, P. Lipari, and T. Stanev, "Cosmic ray interaction event generator SIBYLL 2.1", Physical Review D **80**, 094003, 094003 (2009).

[83] F. Riehn, R. Engel, A. Fedynitch, T. K. Gaisser, and T. Stanev, "Hadronic interaction model SIBYLL 2.3d and extensive air showers", Physical Review D **102**, 063002, 063002 (2020).

[84] T. Kamae, N. Karlsson, T. Mizuno, T. Abe, and T. Koi, "Parameterization of γ, $e^{+/-}$, and Neutrino Spectra Produced by p-p Interaction in Astronomical Environments", The Astrophysical Journal **647**, 692–708 (2006).

[85] S. Koldobskiy et al., "Energy spectra of secondaries in proton-proton interactions", Physical Review D **104**, 123027, 123027 (2021).

[86] Planck Collaboration, "Planck 2018 results. VI. Cosmological parameters", Astronomy and Astrophysics **641**, A6, A6 (2020).

[87] B. Pontecorvo, "Mesonium and Antimesonium", Soviet Journal of Experimental and Theoretical Physics **6**, 429 (1958).

[88] Z. Maki, M. Nakagawa, and S. Sakata, "Remarks on the Unified Model of Elementary Particles", Progress of Theoretical Physics **28**, 870–880 (1962).

[89] B. Pontecorvo, "Neutrino Experiments and the Problem of Conservation of Leptonic Charge", Soviet Journal of Experimental and Theoretical Physics **26**, 984 (1968).

[90]   Super-Kamiokande Collaboration, "Evidence for Oscillation of Atmospheric Neutrinos", *Physical Review Letters* **81**, 1562–1567 (1998).

[91]   SNO Collaboration, "Measurement of the Rate of $\nu\_e + d \rightarrow p + p + e^-$ Interactions Produced by ^{8}B Solar Neutrinos at the Sudbury Neutrino Observatory", *Physical Review Letters* **87**, 071301, 071301 (2001).

[92]   R. C. Gilmore, R. S. Somerville, J. R. Primack, and A. Domínguez, "Semi-analytic modelling of the extragalactic background light and consequences for extragalactic gamma-ray spectra", *Monthly Notices of the Royal Astronomical Society* **422**, 3189–3207 (2012).

[93]   A. Saldana-Lopez et al., "An observational determination of the evolving extragalactic background light from the multiwavelength HST/CANDELS survey in the Fermi and CTA era", *Monthly Notices of the Royal Astronomical Society* **507**, 5144–5160 (2021).

[94]   J. D. Finke et al., "Modeling the Extragalactic Background Light and the Cosmic Star Formation History", *The Astrophysical Journal* **941**, 33, 33 (2022).

[95]   R. J. Protheroe and P. L. Biermann, "A new estimate of the extragalactic radio background and implications for ultra-high-energy γ-ray propagation", *Astroparticle Physics* **6**, 45–54 (1996).

[96]   I. C. Nițu, H. T. J. Bevins, J. D. Bray, and A. M. M. Scaife, "An updated estimate of the cosmic radio background and implications for ultra-high-energy photon propagation", *Astroparticle Physics* **126**, 102532, 102532 (2021).

[97]   A. Addazi et al., "Quantum gravity phenomenology at the dawn of the multi-messenger era-A review", *Progress in Particle and Nuclear Physics* **125**, 103948, 103948 (2022).

[98]   G. Di Marco, R. Alves Batista, and M. Á. Sánchez-Conde, "Revisiting the propagation of highly-energetic gamma rays in the Galaxy", *arXiv e-prints*, arXiv:2408.08818, arXiv:2408.08818 (2024).

[99]   M. G. Hauser and E. Dwek, "The Cosmic Infrared Background: Measurements and Implications", *Annual Review of Astronomy and Astrophysics* **39**, 249–307 (2001).

[100]   A. Kashlinsky, "Cosmic infrared background and early galaxy evolution", *Physics Reports* **409**, 361–438 (2005).

[101]   G. Lagache, J.-L. Puget, and H. Dole, "Dusty Infrared Galaxies: Sources of the Cosmic Infrared Background", *Annual Review of Astronomy & Astrophysics* **43**, 727–768 (2005).

[102]   R. Conn Henry, J. Murthy, J. Overduin, and J. Tyler, "The Mystery of the Cosmic Diffuse Ultraviolet Background Radiation", *The Astrophysical Journal* **798**, 14, 14 (2015).

[103] M. S. Akshaya, J. Murthy, S. Ravichandran, R. C. Henry, and J. Over-duin, "Components of the diffuse ultraviolet radiation at high latitudes", Monthly Notices of the Royal Astronomical Society **489**, 1120–1126 (2019).

[104] B. Welch, S. McCandliss, and D. Coe, "Galaxy Cluster Contribution to the Diffuse Extragalactic Ultraviolet Background", The Astronomical Journal **159**, 269, 269 (2020).

[105] A. Franceschini, G. Rodighiero, and M. Vaccari, "Extragalactic optical-infrared background radiation, its time evolution and the cosmic photon-photon opacity", Astronomy and Astrophysics **487**, 837–852 (2008).

[106] A. Domínguez et al., "Extragalactic background light inferred from AEGIS galaxy-SED-type fractions", Monthly Notices of the Royal Astronomical Society **410**, 2556–2578 (2011).

[107] S. P. Driver et al., "Measurements of Extragalactic Background Light from the Far UV to the Far IR from Deep Ground- and Space-based Galaxy Counts", The Astrophysical Journal **827**, 108, 108 (2016).

[108] F. W. Stecker, S. T. Scully, and M. A. Malkan, "An Empirical Determination of the Intergalactic Background Light from UV to FIR Wavelengths Using FIR Deep Galaxy Surveys and the Gamma-Ray Opacity of the Universe", The Astrophysical Journal **827**, 6, 6 (2016).

[109] A. Cooray, "Extragalactic background light measurements and applications", Royal Society Open Science **3**, 150555 (2016).

[110] R. Hill, K. W. Masui, and D. Scott, "The Spectrum of the Universe", Applied Spectroscopy **72**, 663–688 (2018).

[111] E. Rutherford, "Lxxix. the scattering of α and β particles by matter and the structure of the atom", The London, Edinburgh, and Dublin Philosophical Magazine and Journal of Science **21**, 669–688 (1911)

[112] L. D. Landau and E. M. Lifshitz, *The classical theory of fields*, 4th ed. (Butterworth-Heinemann, Oxford, 1980).

[113] M. Cannoni, "Lorentz invariant relative velocity and relativistic binary collisions", International Journal of Modern Physics A **32**, 1730002, 1730002 (2017).